

Journal Pre-proof

Stratigraphic architecture and paleosols as basin correlation tools of the early Paleogene infill in central–south Patagonia, Golfo San Jorge Basin, Argentinean Patagonia

M. Sol Raigemborn, Elisa Beilinson



PII: S0895-9811(20)30031-6

DOI: <https://doi.org/10.1016/j.jsames.2020.102519>

Reference: SAMES 102519

To appear in: *Journal of South American Earth Sciences*

Received Date: 15 January 2020

Accepted Date: 22 January 2020

Please cite this article as: Raigemborn, M.S., Beilinson, E., Stratigraphic architecture and paleosols as basin correlation tools of the early Paleogene infill in central–south Patagonia, Golfo San Jorge Basin, Argentinean Patagonia, *Journal of South American Earth Sciences*, <https://doi.org/10.1016/j.jsames.2020.102519>.

This is a PDF file of an article that has undergone enhancements after acceptance, such as the addition of a cover page and metadata, and formatting for readability, but it is not yet the definitive version of record. This version will undergo additional copyediting, typesetting and review before it is published in its final form, but we are providing this version to give early visibility of the article. Please note that, during the production process, errors may be discovered which could affect the content, and all legal disclaimers that apply to the journal pertain.

© 2020 Elsevier Ltd. All rights reserved.

1 **Stratigraphic architecture and paleosols as basin correlation tools of the**
2 **early Paleogene infill in central–south Patagonia, Golfo San Jorge Basin,**
3 **Argentinean Patagonia**

4

5 M. Sol Raigemborn^{a,*}, Elisa Beilinson^b

6

7 ^aCONICET – UNLP. Centro de Investigaciones Geológicas, Diagonal 113 n.º
8 275 (1900) La Plata, Argentina, and Cátedra de Micromorfología de Suelos,
9 Facultad de Ciencias Naturales y Museo, UNLP, Calle 122 y 60 s/n, (1900) La
10 Plata, Argentina

11 ^bCONICET – UNLP. Centro de Investigaciones Geológicas, Diagonal 113
12 n.º275 (1900) La Plata, Argentina, and Cátedra de Sedimentología Especial,
13 Facultad de Ciencias Naturales y Museo, UNLP, Calle 122 y 60 s/n (1900) La
14 Plata, Argentina

15

16 * Corresponding author. Tel and Fax: (+54) 221 6441230

17 *E-mail address:* msol@cig.museo.unlp.edu.ar (M.S. Raigemborn)

18

19 Abstract

20

21 The Paleogene infill of the eastern Golfo San Jorge Basin, Patagonia,
22 Argentina, is composed of marine and terrestrial deposits. The latter are fluvial,
23 pedogenically modified successions interlayered with eolian volcanoclastic
24 deposits during the Eocene. Several authors have highlighted the stratigraphic
25 significance and usefulness of strongly developed paleosols in the definition of

26 sequence stratigraphic studies. Even though the area hosts abundant
27 geological and paleopedological data, no large-scale (i.e., basin-scale)
28 stratigraphic architectural correlation including paleosols and relationships
29 within the sequence stratigraphic context had hitherto been carried out. By
30 integrating previously published and unpublished data sets, this paper proposes
31 a sequence stratigraphic framework for the middle Danian–middle Eocene
32 successions of the eastern Golfo San Jorge Basin. Here, spatio-temporal
33 changes in fluvial/alluvial architecture of the Paleogene infill allow us to define
34 four depositional sequences (S), limited by sequence boundaries (SB) that
35 internally presents a low-accommodation system tract (LAST), and a high-
36 accommodation system tract (HAST). Part of these sequences occur as fining-
37 upwards fluvial successions that are pedogenically modified on top by strongly
38 developed paleosols, or are erosively overlain by the coarse-grained base of
39 the following sequence without the development of well-developed paleosols.
40 The sedimentological and paleopedological analysis of the four sequences
41 identified for the early Paleogene infill of the basin indicates that the interplay
42 between subsidence, base level, and climate have controlled both fluvial style
43 and landscape evolution, as well as soil development. Volcaniclastic supply also
44 played a significant role, especially during the Eocene.

45

46 *Keywords:* Río Chico Group; Non-marine Sequence Stratigraphy; System
47 Tracts; Ultisol-like paleosols; Allogenic Controls

48

49 1. Introduction

50

51 The development of an integrated model that includes paleosols, fluvial
52 facies, and the associated bounding surfaces is crucial to the prediction of non-
53 marine stratigraphic architecture (e.g., Wright and Marriott, 1993; Kraus, 1999;
54 Varela et al., 2012; Ashley et al., 2013; Beilinson et al., 2013; McCarthy and
55 Plint, 2013; Amorosi et al., 2014; 2017, among others). Fluvial-alluvial systems
56 may respond to a variety of allogenic controls such as eustasy, climate,
57 tectonics, and basin subsidence, and the relative impact of these in the resulting
58 architecture can be identified (e.g., Wright and Marriott, 1993; Shanley and
59 McCabe, 1994). Particularly, paleosols represent a powerful tool for
60 stratigraphic correlation in alluvial deposits (Bown and Kraus, 1987; Wright and
61 Marriott, 1993; Kraus, 1999, among others) because they can be used as
62 regional stratigraphic markers to trace genetic packages across sequence-
63 bounding unconformities at different scales (e.g., Demko et al., 2004; Amorosi
64 et al., 2014). Another notable application of the paleosols is that their temporal
65 evolution, recorded by the change in the dominant pedofeatures, attests for
66 base-level changes (e.g., Kraus et al., 1999; Catuneanu, 2006). Theoretically,
67 paleosol types change with a fluctuating base level, allowing them to assess
68 their relative importance/significance from a sequence stratigraphic viewpoint
69 (Wright and Marriott, 1993; Catuneanu, 2006). From this perspective, paleosols
70 provide key evidence for the reconstruction of syndepositional conditions during
71 the accumulation of system tracts, or the temporal significance of stratigraphic
72 hiatuses related to sequence-boundary unconformities. Thus, more developed
73 or mature paleosols form either during stages of non-deposition or erosion and
74 in association with sequence boundaries; on the contrary, less developed or
75 immature paleosols and generally aggrading ones (i.e., compound, composite,

76 cumulative following Kraus, 1999) take place during stages of sediment
77 accumulation associated with the deposition of sequences (e.g., Catuneanu,
78 2006).

79 Outcrop exposures of the early Paleogene succession of the Golfo San
80 Jorge Basin (GSJB) located in central Argentinean Patagonia, represent an
81 excellent opportunity to verify the benefits of the paleosols in stratigraphy as
82 well as to examine the distribution of depositional systems and the stacking
83 patterns of marine and terrestrial sequences. The eastern area of the GSJB
84 (North Flank, Center of the Basin, and South Flank; Fig. 1A) has a conspicuous
85 background of stratigraphic information of the early Danian marine–estuarine
86 Salamanca Formation and the overlying middle Danian–middle Eocene fluvial–
87 alluvial and eolian deposits, in part bearing paleosols, of the Río Chico Group
88 (Fig. 2). The area hosts abundant sedimentological and paleopedological data
89 (Feruglio, 1949; Andreis et al., 1975; Legarreta et al., 1990; Martínez, 1992;
90 Legarreta and Uliana, 1994; Matheos et al., 2001; Iglesias, 2007; Raigemborn,
91 2008; Raigemborn et al., 2009a, b, 2010, 2014, 2018a, b; Krause et al., 2010a,
92 b, 2017; Krause and Piña, 2012; Foix et al., 2013, 2015; Clyde et al., 2014;
93 Woodburne et al., 2014; Comer et al., 2015; Ruiz et al., 2017, 2020; Lizzoli et
94 al., 2018; Zucol et al., 2018), at which recently was added a temporal resolution
95 (Clyde et al., 2014; Krause et al., 2017). The Salamanca Formation and the
96 lowermost Río Chico Group have been recently correlated with globally
97 recognized sea-level events, highlighting the role of fluctuating sea level as a
98 primary control (e.g., Clyde et al., 2014; Comer et al., 2015). On the other side,
99 outcrops and subsurface data of the Salamanca Formation and the Río Chico
100 Group at the North Flank of the basin have been related to changes in

101 accommodation space and to differential subsidence across the basin (Foix et
102 al., 2013, 2015). However, up to date, no large-scale (i.e., basin-scale)
103 stratigraphic architectural correlation, including paleosols and relationships
104 within the sequence stratigraphic context of both the Salamanca Formation and
105 the Río Chico Group, have hitherto been carried out. Consequently, the aims of
106 this research are 1) to analyze spatio-temporal changes in depositional
107 environments, paleosol types, and total thickness of the Río Chico Group,
108 making correlations throughout the eastern part of the GSJB (see Fig. 1A and
109 B), and 2) to construct a sequence stratigraphic scheme for the middle Danian–
110 middle Eocene successions of this part of the basin.

111

112 2. Geological context

113

114 The GSJB is an extensional intracontinental basin located in southern
115 Argentina that developed on Paleozoic continental crust linked to the
116 Gondwana break-up (e.g., Fitzgerald et al., 1990). It suffered different phases of
117 extensional reactivation during the Cretaceous, followed by the process of
118 positive inversion tectonics along the San Bernardo Fold Belt (Fig. 1A), which
119 rose mainly during the Neogene (Homoc et al., 1995; Paredes et al., 2018).
120 Figari et al. (1999) internally divided this basin according to its structural style
121 into five zones: North Flank, Center of the Basin, South Flank, San Bernardo
122 Fold Belt, and Western Sector (Fig. 1A). Using the Figari's scheme, which was
123 defined to the Castillo Formation, our research is mainly placed in the Eastern
124 Sector of the basin (i.e., North Flank, Center of the Basin, and South Flank)
125 (Fig. 1A and B), where an extensional style prevails (Figari et al., 1999;

126 Giampaoli, 2015). However, the locality of Cerro Abigarrado (Fig. 1A and B) is
127 located on the less deformed eastern margin of the San Bernardo Fold Belt,
128 where Gianni et al. (2017) indicated that a contractional tectonic regime took
129 place during the Eocene. Paleogeographic reconstructions consider the Eastern
130 Sector of the GSJB as a large engulfment with W-E orientation open to the
131 Atlantic Ocean (e.g., Malumián et al., 1999; Malumián and Nañez, 2011;
132 Gomez Peral et al., 2019).

133 The earliest Cenozoic infill of the GSJB is characterized by a near-
134 horizontal succession of marine and continental sedimentary rocks deposited in
135 a passive margin setting in an extensional context (e.g., Figari et al., 1999; Foix
136 et al., 2008, 2012), exceeding the Cretaceous boundaries of the Chubut Group
137 basin (Foix et al., 2015). This infill starts with the marine–estuarine deposits of
138 the Salamanca Formation, which correspond to an Atlantic transgression that
139 flooded the Eastern Sector of the basin during the Danian (Fig. 2). The
140 Salamanca Formation is stratigraphically composed of five sections known as
141 Lignitífero, Glauconítico, Fragmentosa, Banco Verde, and Banco Negro Inferior
142 (in stratigraphic order, according to Feruglio, 1949). In the westernmost North
143 Flank and the surroundings of the San Bernardo Fold Belt, the Salamanca
144 Formation was deposited during the early Danian; instead, farther east, it has
145 been assigned to be middle-late Danian (Clyde et al., 2014). The Salamanca
146 Formation was covered during the middle Danian by the continental deposits of
147 the Río Chico Group, that persisted active up to the middle Eocene (following
148 Clyde et al., 2014; Krause et al., 2017; Raigemborn et al., 2018a) (Fig. 2).
149 Internally, the Río Chico Group is composed of four units that, from the oldest to
150 the youngest, are Las Violetas, Peñas Coloradas, Las Flores, and Koluel-Kaike

151 formations (Raigemborn et al., 2010). Deposition of the Río Chico Group took
152 place in the Eastern Sector of the basin and in the vicinity of the San Bernardo
153 Fold Belt and the Deseado Massif to the south (Fig. 1). The tectonic setting of
154 the Río Chico deposits is still debated, while field information in the eastern of
155 the basin attest to deposition during extension (Foix et al., 2013), outcrop data
156 point out to syntectonic deposition of the Koluel-Kaike Formation to the west
157 and south of the San Bernardo Fold Belt, suggesting a contractional regime
158 (Gianni et al., 2017). The Río Chico Group is overlain by marine and continental
159 units that represent the middle-late Cenozoic infill of the basin (Fig. 2).

160 The localities selected for this paper, based on the presence of early
161 Cenozoic outcrops, along the Eastern Sector of the GSJB and the eastern
162 margin of the San Bernardo Fold Belt (Patagonia, Argentina; Fig. 1A and B) are:
163 Estancia Las Violetas, Punta Peligro–Estancia La Rosa (Rocas Coloradas
164 area), Cañadón Hondo area, Estancia La Campanita–Gran Barranca (Las
165 Flores area), Cerro Blanco, Bosque Ormaechea (Cerro Abigarrado area),
166 Cañadón Lobo, Río Deseado area, and Laguna Manantiales (from north to
167 south; see Fig. 1B). An integrated stratigraphic chart is provided in Figure 2 to
168 correlate studied lithostratigraphic units throughout the different localities of the
169 basin.

170 In the northeastern area of the North Flank (Estancia Las Violetas–Rocas
171 Coloradas; see Fig. 1B), the Salamanca Formation outcrops start with the
172 Glauconítico and Fragmentosa deposits, which are followed by the estuarine
173 deposits of the Banco Verde and the pedogenized swamp deposits of the
174 Banco Negro Inferior (BNI) (Feruglio, 1949; Andreis et al., 1975; Legarreta et
175 al., 1990; Legarreta and Uliana, 1994; Raigemborn, 2008; Raigemborn et al.,

2010, 2014; Foix et al., 2015; Ruiz et al., 2017, this volume). The Río Chico Group in this area comprises the low-sinuosity fluvial systems of the Las Violetas Formation, the moderate- to high-sinuosity fluvial systems of the Peñas Coloradas Formation, and the moderate- to high-sinuosity fluvial systems of the Las Flores Formation (Feruglio, 1949; Andreis et al., 1975; Legarreta et al., 1990; Legarreta and Uliana, 1994; Raigemborn, 2008; Krause, 2009; Raigemborn et al., 2010, 2014; Krause and Piña, 2012; Foix et al., 2013, 2015). Foix et al. (2013, 2015) related the first of these fluvial architectures to a high aggradation rate, and to a low aggradation rate to the latter, and attributed both styles to variations in subsidence rates and sedimentary supply, assuming a constant climate across the Golfo San Jorge Basin. The Las Violetas and Peñas Coloradas formations show a lateral stratigraphic relationship (Raigemborn et al., 2010; Krause et al., 2017). However, a significant erosional unconformity separates the Las Flores Formation from the underlying Peñas Coloradas (e.g., Legarreta and Uliana, 1994; Krause et al., 2017). Both the age and the regional extent of the basal unconformity over which the Las Flores Formation lies suggest that this surface could have been caused by an erosive event related to a fall in base level. One possible origin of this unconformity could be the effects of global eustatic sea-level fall near the Paleocene–Eocene boundary (ca. 56 Ma) (Krause et al., 2017).

In the southwestern part of the North Flank and the eastern margin of the San Bernardo Fold Belt (Las Flores and Cerro Abigarrado areas, respectively; see Fig. 1B), the Salamanca Formation is represented by the marine–estuarine and coastal swamps deposits of the Glauconítico–Banco Negro Inferior (Feruglio, 1949; Legarreta et al., 1990; Martínez, 1992; Legarreta and Uliana,

1994; Matheos et al., 2001; Iglesias, 2007; Raigemborn, 2008; Raigemborn et al., 2010, 2014; Clyde et al., 2014; Comer et al., 2015). The Río Chico Group is represented by the fluvial deposits of the Peñas Coloradas, Las Flores, and the pedogenically modified fluvial Koluel-Kaike Formation (Raigemborn, 2008; Krause et al., 2010, 2017; Raigemborn et al., 2010, 2014; Clyde et al., 2014; Woodburne et al., 2014; Comer et al., 2015). Taking these into consideration, Clyde et al. (2014) and Comer et al. (2015) proposed a general sequence stratigraphic framework for the Salamanca Formation and the lower Río Chico Group (i.e., Peñas Coloradas Formation) deposits of the area. These authors recognized an erosional surface between the Banco Negro Inferior and the Peñas Coloradas Formation and sedimentary systems tracts, and combined them with chronologic data and the global eustatic sea-level curve. In this context, the Banco Negro Inferior is interpreted as a highstand system tract that overlays the late transgressive one of the upper Banco Verde. A eustatic sea-level fall gave place to a sequence boundary that separates the Banco Negro Inferior from the Peñas Coloradas Formation, which also represents the end of the early Paleogene marine sedimentation in the basin.

Although in the Center of the Basin and most of the South Flank (see Fig. 1B) the Salamanca Formation and the Río Chico Group occur at subsurface (e.g., Fitzgerald et al., 1992; Figari et al., 1999; Hechem and Strelkov, 2002; Paredes et al., 2015), towards the south of the South Flank (Río Deseado area and Laguna Manantiales; see Fig. 1B) both units are outcropping. The outcrops of the Salamanca Formation are restricted to the Banco Verde–Banco Negro Inferior (Raigemborn et al., 2018b); meanwhile, the Río Chico Group comprises the outcrops of the fluvial Las Flores Formation and the distal eolian-dominated

226 fluvial Koluel-Kaike Formation, both of them pedogenically modified (Lizzoli et
227 al., 2018; Raigemborn et al., 2018a, b).

228

229 3. Methodology

230

231 Although a significant part of the early Cenozoic deposits is in the
232 subsurface of the South Flank and the Center of the Basin, in this study, we
233 carry on a revision of the latest works dealing with the Paleogene
234 sedimentology based on outcrop data of the Eastern Sector of the GSJB. Here
235 we include our own and bibliographic information (see previously), covering the
236 east of the GSJB (i.e., the North Flank and the South Flank) (Fig. 1B).

237 We consider spatio-temporal changes in facies, facies associations,
238 fluvial styles, the geometry of fluvial-alluvial bodies, preservation of floodplain
239 deposits, paleosols, and thickness of the units throughout the study area to
240 define the early Cenozoic stratigraphic architecture of the GSJB.

241 Facies were described following Miall's (1996) and Bridge's (2003)
242 schemes but adapted to volcanoclastic successions (Table 1). The terms
243 tuffaceous sandstones, siltstones, and mudstones were respectively used for
244 reworked sand-, silt-, and mud-sized pyroclastic sediments with sporadic
245 reworked epiclastic grains. Facies associations were described following Miall's
246 (1996) scheme (Table 1).

247 Paleosols were identified in outcrop based on macroscopic pedofeatures,
248 such as structure, mottles, nodules, color, slickensides, burrows, and rhizoliths
249 (e.g., Retallack, 2001). Colors were described according to the Munsell notation
250 (Munsell Soil Color Book, 2013). In paleosol horizons, thickness, contact types,

251 mineral composition, mean grain size, ped structure, type of nodules, and
252 evidence of bioturbation were described (e.g., Soil Survey Staff 1999; Retallack,
253 2001). Classification of the paleosols was made following the criteria of USDA,
254 Soil Taxonomy (1975, 1998), and the modifications for paleosols by Retallack
255 (1994). Some of these items are summarizing in Tables 1 and 2. The description
256 of pedofeatures at macroscale together with the differentiation of the soil
257 horizons, the interpretation of main soil-forming processes, and the paleosols
258 classification served as the basis for the definition of very weakly, weakly,
259 strongly, and very strongly developed paleosols (see Table 2). The well-
260 exposed and the great lateral continuity of the paleosols-bearing outcrops of the
261 Río Chico Group in the study area allowed an analysis of the laterally
262 continuous paleosols within the unit. Thus, using a combination of macroscopic
263 properties of the different types of paleosols identified and their stratigraphic
264 position throughout the Río Chico Group, a large-scale correlation can be
265 established, and for this reason, they represent powerful stratigraphic markers
266 within the study unit. In this sense, we give special consideration to the
267 identification and lateral tracing of strongly- and very strongly-developed
268 paleosols as key surfaces on a regional scale. Very weakly and weakly-
269 developed paleosols (i.e., Entisol-, Andisol-, and Inceptisol-like paleosols; Table
270 2) within the Río Chico Group were observed as laterally discontinuous, and
271 given a different hierarchical value than the more mature ones (i.e., paleosols
272 with strong–very strong degree of development), and consequently, we do not
273 consider them as key surfaces. Unlike, intensely modified beds that are laterally
274 continuous represent key markers for our high-resolution stratigraphic analysis
275 of the GSJB. Strongly- and very strongly-developed paleosols (i.e., Alfisol-,

276 Ultisol- and Ultisol-like paleosols with plinthitic horizon and equivalent paleosols,
277 and Aridisol-like paleosols with calcic horizon; Table 2) suggest temporal
278 persistence of broadly similar soil-forming conditions as the entire soil sequence
279 developed. On the contrary, very weakly-developed paleosols reflect cessation
280 of sedimentation for only a very short–short period of time (e.g., Retallack,
281 2001). In the study area, regionally extensive paleosols are the dominant
282 stratigraphic markers at the westernmost North Flank and the South Flank
283 (basin margin), while channel/floodplain cycles are the main key markers in the
284 eastern North Flank.

285 In order to simplify previous sedimentological and paleopedological
286 results, we selected the most complete succession of the Río Chico Group for
287 each studied area of the GSJB. Although data from these sections are original,
288 some sedimentological details were taken from the literature to complement our
289 observations. Thus, the profile of the Estancia Las Violetas locality is the
290 representative for the eastern North Flank (Figs. 1B and 3); the composite
291 section of the Punta Peligro–Estancia La Rosa (Rocas Coloradas area)
292 represents the coastal area of the North Flank (Figs. 1B and 3); the composite
293 section of the Estancia La Campanita–Barranca Colhué Huapi (Las Flores area)
294 characterizes the western North Flank (Figs. 1B and 3), and the profiles of the
295 Río Deseado area and Laguna Manantiales are the characteristics of the
296 southern and southernmost South Flank (Figs. 1B and 3). Other localities
297 mentioned in the text are shown in Fig. 1B.

298 The chronostratigraphic framework used in this paper was following
299 Clyde et al. (2014) and Krause et al. (2017) for the Salamanca Formation and

300 the Río Chico Group, and following Ré et al. (2010) and Dunn et al. (2013) for
301 the lower Sarmiento Formation (see Fig. 2).

302

303 4. Results: Sequence stratigraphy

304

305 After the marine withdrawal at the end of Salamanca Formation (Banco
306 Negro Inferior), continental conditions developed during the accumulation of the
307 Río Chico Group deposits. In this context, the absence of marine or
308 contemporary coastline deposits makes it difficult to use classical sequence
309 stratigraphical terminology. In order to solve this, we will use Dahle et al. (1997)
310 sequence stratigraphic approach, and introduce the high- and low
311 accommodation system tracts, which are defined mainly based on facies
312 associations present in the succession, also taking into account the relative
313 proportion of channel deposits and floodplain deposits. Each of these systems
314 tracts refers to periods in which there was an increase or decrease in the rate of
315 generation of accommodation (Dahle et al., 1997; Catuneanu, 2006). They refer
316 to tendencies in accommodation and sedimentation with no implications for
317 relative sea level.

318 For the early Paleogene deposits of the eastern GSJB, the correlation of
319 the facies association between the studied outcrops revealed the stratigraphic
320 architecture (Fig. 3). Independently of the lithostratigraphic data (i.e., without
321 taking in consideration the limits previously assigned to the stratigraphic units),
322 we divided the Río Chico Group into four intervals: lower, middle, upper, and
323 uppermost, all of them separated by erosive surfaces (Figs. 4–6). Thus, each of
324 these intervals defines a sequence (S1, S2, S3, S4), limited by sequence

325 boundaries (SB1, SB2, SB3, SB4, SB5), that internally presents a low-
326 accommodation system tract (LAST1, LAST2, LAST3, LAST4), and a high-
327 accommodation system tract (HAST1, HAST2, HAST3, HAST4) (Figs. 4–6).

328

329 4.1. Sequence 1 (S1)

330

331 Sequence 1 corresponds to the lower part of the Río Chico Group,
332 including Las Violetas and Peñas Coloradas formations (Fig. 4). These are
333 continental deposits that overlay the swamp deposits of the Banco Negro
334 Inferior (Salamanca Formation) and were interpreted by Clyde et al. (2014) and
335 Comer et al. (2015) as lowstand systems tract deposits following late
336 transgressive/highstand system tract deposits.

337 The basal boundary of the S1 (sequence boundary 1; SB1) is
338 represented by an irregular or plane and erosional surface marked by the basal
339 surface of the channels belonging to either the Las Violetas (Estancia Las
340 Violetas and Cañadón Hondo; Fig. 1B) or the Peñas Coloradas Formation
341 (Rocas Coloradas area, Las Flores area, Cerro Abigarrado; Figs. 1B),
342 depending on the area (Figs. 3, 4 and 5A, B). Usually, this surface incises the
343 upper part of the Salamanca Formation, but at the western North Flank (Las
344 Flores area) (Fig. 1B), the SB1 erodes down to the Banco Verde of the
345 Salamanca Formation (Iglesias, 2007).

346 After the development of the SB1, the LAST1 deposits were accumulated
347 (Figs. 4 and 5A, B). These are represented by 16 to 30 m of very coarse- and
348 coarse-grained fining-upward successions ranging from greenish-gray epiclastic
349 and tuffaceous conglomerates to coarse- and medium-grained sandstones
350 (facies Gm, Gt, Gp, St, Sp, Sm, Se, Sl of the FA1 and FA2; see explanation of

351 these codes in Table 1). Such deposits were interpreted by Foix et al. (2013,
352 2015) as braided channels and as a low- and moderate- to high-sinuosity fluvial
353 system with mixed load (sandy-gravelly), where the channels would be multiple
354 and mobile by Raigemborn et al. (2010; 2014). Fine-grained (sandy-muddy)
355 tabular beds of St, Sr, Sm, Sl, Fm, and Fl facies (FA4 and FA5; see an
356 explanation of these codes in Table 1) with sporadic paleosols with a very weak
357 degree of development are interbedded into this coarser facies (Fig. 3; Table 2).

358 The LAST1 is followed by the HAST1 (Figs. 3, 4 and 5A, B, E), which is
359 characterized by 12 to 50 m of stacking tabular bodies composed of gray to
360 orange-reddish tuffaceous sandy-siltstones (St, Sm, Sr, Sl, Fm, Fl, TSm, TMb
361 and TMm of the FA3, FA4 and FA5; see explanation of these codes in Table 1)
362 interpreted as sheet-flood deposits, distal floodplain deposits, and in less
363 proportion as proximal floodplain deposits, respectively (Raigemborn et al.,
364 2009, 2014). Paleosols with very weak- to strong-degree of development
365 (Entisols, Inceptisols, and Alfisols; see Table 2) developed over such deposits
366 (Krause et al., 2010b; Raigemborn et al., 2009b) (Figs. 3, 4, 5A, and 6A, B).
367 Channel-fill deposits are absent in the HAST1.

368

369 At the South Flank of the basin, there are no outcrops assigned to
370 deposits of the Las Violetas and/or Peñas Coloradas formations (see below)
371 (Fig. 4).

372

373 4.2. Sequence 2

374

375 The contact between S1 and S2 is characterized by an erosive and
376 irregular surface (SB2) (Figs. 4 and 5C–E). Lithostratigraphically, this surface
377 corresponds to the contact between the Salamanca Formation or Las
378 Violetas/Peñas Coloradas formations and the Las Flores Formation, and it can
379 be followed through the outcrops of the northern and southern part of the study
380 area (e.g., Raigemborn et al., 2010, 2018b; Krause et al., 2017) and in the
381 subsurface in the Center of the basin (Legarreta and Uliana, 1994). Thus, this
382 surface is regionally extended throughout the study area. Notably, in the
383 southernmost of the GSJB, the SB2 is an erosional and discordant surface
384 developed between the deposits of the Banco Verde–Banco Negro Inferior
385 (Salamanca Formation) and the Las Flores Formation (Figs. 3 and 5C).

386 The LAST2 comprises 25 to 30 m of pinky to grayish or orangey and
387 whitish coarse-grained facies (Gm, Gt, St, Sp, Se facies; see an explanation of
388 these codes in Table 1) interpreted as sandy-gravelly low- and moderate- to
389 high- sinuosity fluvial channels (FA1 and FA2; Table 1) (Raigemborn et al.,
390 2010, 2014; Foix et al., 2013, 2015), interbedded with thin packages of fine-
391 grained bodies corresponding to distal floodplain deposits (Foix et al., 2013,
392 2015). These last beds are mainly epiclastic and in less proportion
393 volcanoclastic in composition (Fm, and TMm facies; see an explanation of these
394 codes in Table 1), and are interpreted mainly as distal floodplain deposits
395 (Raigemborn et al., 2018b) (FA5; Table 1). At the Rocas Coloradas area, the
396 LAST2 is cover concordantly by pedogenically modified white tuffaceous
397 deposits assigned to the Gran Barranca Member of the Sarmiento Formation
398 (Krause and Piña, 2012).

399 In the north North Flank (Estancia Las Violetas; Fig. 1B), the HAST2 is
400 characterized by c.10 m of reddish–brownish tabular muddy bodies (Fm facies;
401 see an explanation of this code in Table 1) interpreted as distal fluvial floodplain
402 areas (FA5, Table 1) which are eroded by the shallow marine deposits of the
403 Miocene Chenque Formation (Figs., 3, 4 and 5A). Towards the west (Las Flores
404 area), the HAST 2 is represented by 30 to 44 m of grayish–greenish
405 homogeneous muddy deposits, epiclastic and volcanoclastic in composition (Fm,
406 Fl, TSm, Tmb, and TMm facies; see an explanation of these codes in Table 1),
407 interpreted as sheet-flood deposits (FA3, Table 1) and distal fluvial floodplain
408 settings (FA5, Table 1) (Fig. 5F) (Raigemborn et al., 2009a and b, 2010, 2014;
409 Woodburne et al., 2014; Krause et al., 2017). Paleosols with very weak- to
410 weak-degree of development are recorded (see Table 2 and Fig. 6C). However,
411 in the middle-upper part of the Las Flores Formation at Las Flores area, Krause
412 et al. (2017) described a condensed section with the occurrence of orange and
413 red beds, interpreted as paleosols that could imply duration of c. 2 m.y. (Fig.
414 6D). These are strong–very strong developed paleosols, and we interpret them
415 as the next sequence boundary (SB3; see below and Fig. 4). In the
416 southernmost South Flank (Laguna Manantiales; Fig. 1B), the HAST2 deposits
417 are practically absent, and instead strongly and very strongly developed Ultisol-
418 and Oxisol- like paleosols (Lizzoli et al., 2018; Raigemborn et al., 2018b) (Table
419 2) developed (Figs. 3, 4, 5C and 6E).

420

421 4.3. Sequence 3

422

423 S3 corresponds to the upper part of the Las Flores Formation and the
424 lower Koluel-Kaike Formation (following Krause et al., 2017) (Figs. 3, 4, 5F, and
425 6D). The contact (SB3) between S2 and S3 is only recorded in the western
426 North Flank (Las Flores area and Cerro Blanco; Figs. 1B, 5F and 6D) and the
427 south of the South Flank of the basin (Laguna Manantiales; Figs. 1B and 5C),
428 where is defined by the occurrence of very strongly developed Ultisol-like
429 paleosol with a plinthitic horizon (Raigemborn et al., 2018) or equivalents (Table
430 2 and Figs. 3, 4, 5C, 6D, F).

431 Overlying this paleosol surface, the LAST3 is represented by c. 5 to 30 m
432 of mainly volcanoclastic fine-grained deposits (TMb, TSm, and TSt facies; see
433 an explanation of these codes in Table 1) corresponding to unconfined (i.e.,
434 sheet-flood, FA3, Table 1) and confined (i.e., low hierarchy fluvial channels,
435 FA6, Table 1). Such levels transition to the HAST3 deposits, represented by
436 tephric loessites (TMm facies, FA7; see an explanation of these codes in Table
437 1), and shallow ponded areas (TMI facies, FA8; see an explanation of these
438 codes in Table 1) (Krause et al., 2010, 2017; Raigemborn et al., 2018 a, b)
439 (Figs. 3, 4 and 5C). LAST3 and HAST3 deposits show pedogenic modification
440 (Fig. 5C), which at western North Flank (Las Flores area–Cerro Blanco) and
441 South Flank (Río Deseado area–Cañadón Lobo) presents a vertical trend from
442 very weakly developed paleosols to very strongly developed ones, and that
443 upwards the trend is reversed (Table 2; see a discussion about this trend in
444 Krause et al., 2010 and Raigemborn et al., 2018a).

445

446 4.4. Sequence 4

447

448 Similarly to the Sequence 3, the contact between S3 and S4 is only
449 evident towards the west of the North Flank (Las Flores area and Cerro Blanco;
450 Fig. 1B) and the south of the South Flank (Río Deseado area and Cañadón
451 Lobo; Fig. 1B). SB4 (Figs. 4 and 6D) is characterized as a non-erosive
452 discontinuity related to long-time pedogenesis, and it is defined by the presence
453 of very strongly developed paleosols (Ultisol-like paleosols with plinthitic horizon
454 and equivalents; Table 2) weathered on top of fine-grained volcanoclastic beds
455 (TMm facies; see an explanation of this code in Table 1) of tephric loessites of
456 the HAST3 (FA7; Table 1) (Fig. 4).

457 Overlying this surface, the LAST4 (Fig. 4) is represented by a succession
458 of c. 5 to 30 m of fine-grained volcanoclastic beds (TMm, TSm, and TMI facies;
459 see an explanation of these codes in Table 1) that correspond to sheet-flood
460 deposits, tephric loessites, and shallow ponded areas (FA3, FA6, and FA7,
461 respectively; see Table 1) (Krause et al., 2010, 2017; Raigemborn et al., 2018
462 a, b). Frequently, these levels are modified by pedogenesis into weakly
463 developed paleosols (Table 2).

464 The HAST4 (Fig. 4) is represented by c. 60 m of pedogenically modified
465 whitish tuffaceous deposits of the Gran Barranca Member (Lower Sarmiento
466 Formation), which cover in gradational contact to the underlying Koluel-Kaike
467 Formation (Bellosi, 2010a, b; Krause et al., 2010, 2017; Raigemborn et al.,
468 2010) (Fig. 6F). These deposits correspond to tephric loessites and ephemeral
469 ponded areas over which very weakly to weakly developed paleosols were
470 formed (Bellosi, 2010a, b; Bellosi and González, 2010; see Fig. 20.3 in Bellosi
471 and González, 2010). These deposits are overlaid by the strongly developed
472 Aridisol-like paleosol with calcic horizon (Table 2) of the Rosado Member. The

473 top of this paleosol was assigned to a high hierarchy by Bellosi (2010b),
474 representing a sequence boundary (SB5; Fig. 4) that involved prolonged
475 subaerial exposure and pedogenesis.

476

477 5. Discussion

478

479 Fluvial systems respond to allogenic controls such as base level, climate,
480 tectonics, basin subsidence, and volcanic supply modifying the basin-fill
481 architecture (e.g., Wright and Marriott, 1993; Shanley and McCabe, 1994
482 Paredes et al., 2007; Amorosi et al., 2017, among others) at low frequencies
483 (10^4 – 10^6 yr) (e.g., Miall, 1996). Changes in the fluvial architecture of the Río
484 Chico Group in the northeast of the GSJB, based on outcrops and subsurface
485 data, have been associated with variations in aggradation, accommodation, and
486 subsidence rates. Although Foix et al. (2013, 2015) have highlighted the role of
487 tectonics as a primary control on sedimentation, Raigemborn et al. (2014,
488 2018a) have also pointed out the role of climate and volcanic input as
489 controlling factors.

490 Spatio-temporal changes in the fluvial architecture of the Río Chico
491 Group in the eastern realm of the GSJB are here recognized (see Fig. 3). In this
492 paper, the early Paleocene–middle Eocene deposits were grouped in four
493 depositional sequences (S1–S4). Part of these sequences occur as fining-
494 upwards fluvial successions that are pedogenically modified on top by strongly-
495 developed paleosols (e.g., Alfisol-like paleosols at the top of the Las Violetas
496 Formation at Estancia Las Violetas), or they are erosively overlain by the

497 coarse-grained base of the following sequence without the development of well-
498 developed paleosols (e.g., lower Las Flores Formation at Las Flores area).

499 Non-marine sequence bounding unconformities record null to negative
500 accommodation/sediment supply rate (A/S ratio), and are defined as regional
501 surfaces of non-deposition and associated subaerial erosion, marking an abrupt
502 change in channel/floodplain ratio or recorded as strongly-developed or mature
503 paleosols that can be traced laterally on a broad scale (e.g., Wright and
504 Marriott, 1993). Sequence boundaries (SB) can be placed at the top of these
505 paleosols because they represent a hiatus in sedimentation and the pedogenic
506 modification of the depositional surface (e.g., Di Celma et al., 2015). Within the
507 analyzed units, five sequence boundaries (SB1–SB5) were recognized (see Fig.
508 4), two of them related to fluvial incision (SB1 and SB2) and the remaining three
509 related to mature paleosols (SB3, SB4, and SB5), and can be described as
510 follows. On a regional scale, the SB1 is an erosional surface that separates the
511 coastal swamp deposits of the Banco Negro Inferior (upper Salamanca
512 Formation) from the fluvial ones of the lower Río Chico Group (Las
513 Violetas/Peñas Coloradas formations) (see Fig. 4). This unconformity records a
514 landward shift in depositional environments and, following Clyde et al. (2014), a
515 gap of c. 1 my in the stratigraphic record. Clyde et al. (2014) and Comer et al.
516 (2015) correlated this erosional surface with a eustatic sea-level fall. This
517 unconformity has a variable erosional relief on underlying strata that at Rocas
518 Coloradas area reaches its maximum of 8 m. However, there is no evidence of
519 the development of incised valleys. In the here analyzed area, the SB2 is a
520 regionally extended erosional surface that has a lower relief of 2–3 m. It occurs
521 between the upper deposits of the Salamanca Formation (Banco Verde–Banco

522 Negro Inferior) or the lower ones of the Río Chico Group (Las Violetas or Peñas
523 Coloradas formations) and the fluvial beds of the Las Flores Formation (see Fig.
524 4). Krause et al. (2017) point out that this surface could have been caused by
525 an erosive event related to a global eustatic fall near the Paleocene-Eocene
526 boundary. On the other side, SB3, SB4, and SB5 are related to very strongly-
527 developed paleosols, which features suggest long geomorphological stability,
528 subaerial exposure and pedogenesis under warm and seasonal humid climatic
529 conditions for SB3 and SB4 (Krause et al., 2010, 2017; Raigemborn et al.,
530 2018a, b), and semi-arid to arid and temperate climatic conditions for the SB5
531 (Bellosi and González, 2010). The Río Chico Group was deposited in
532 coincidence with the Early Paleogene Greenhouse World (e.g., Raigemborn et
533 al., 2009, 2014, 2018a), during which two hyperthermal events and several
534 thermal events took place (Zachos et al., 2001, 2008). The change from Ultisol-
535 like paleosols with plinthitic horizon and equivalent paleosols (SB3 and SB4) to
536 Aridisol-like paleosols with calcic horizon (SB5) could reflect the transition from
537 greenhouse to icehouse world, which establishes at the Eocene-Oligocene
538 boundary. Stratigraphic correlation of the very strongly developed paleosols of
539 the middle part of the Las Flores Formation over distances of hundreds of
540 kilometers (see Las Flores area and Laguna Manantiales in Fig. 1B) and across
541 different fluvial/alluvial domains suggests an external forcing on paleosols
542 development. Climate and a low base level were probably the main allogenic
543 controlling factors. Krause et al. (2017) and Raigemborn et al. (2018b)
544 suggested a link between these mature paleosols with the early Eocene Climate
545 Optimum (51–53 Ma; Zachos et al., 2008). Similarly, stratigraphic correlation of
546 strongly and very-strongly developed paleosols of the Koluel-Kaike Formation

547 over hundreds of kilometers (see Las Flores area, Río Deseado area, Cañadón
548 Lobo, and Laguna Manantiales in Fig. 1B), point in the same direction. Thus,
549 the lateral persistence of these paleosols types (Ultisol- and Ultisol-like
550 paleosols with plinthitic horizon) suggests similar spatial climate conditions.

551 Changes in sediment supply to the fluvial/alluvial systems can be
552 controlled by both river dynamics and by climate conditions that influence the
553 vegetation cover on the slopes and their erosion (e.g., Di Celma et al., 2015;
554 Opluštil et al., 2015). Colder and drier conditions could led to the formation of
555 low-accommodation system tracts when rates of sediment supply are high and
556 accommodation space is low; whereas warmer and wetter conditions allow the
557 development of high-accommodation system tracts, when rates of generation of
558 accommodation space are higher than sediment supply rates. Within the
559 studied HAST's, several paleosols with very weak to weak degree of
560 development or immature paleosols were developed, representing short
561 intervals of landscape stability ($<10^2$ – 10^3 yr; Raigemborn et al., 2018a). These
562 paleosols types might represent the effect of climatic variations, with successive
563 short-time spans of soil development alternating with periods of
564 geomorphological instability, aggradation phases with continuous and rapid
565 deposition (e.g., Marriott and Wright, 1993; Amorosi et al., 2017; Raigemborn et
566 al., 2018a).

567 At a sequence scale, fluvial/alluvial architecture reflects changes in
568 accommodation space. Sequences are represented at their base by braided or
569 laterally amalgamated fluvial channels with null o very low preservation of fine-
570 grained floodplain deposits (LAST's), which become ribbon-like channel beds
571 encased in fine-grained floodplain deposits and finally only floodplain deposits,

572 with no channel development (HAST's). The contact between the LAST and the
573 HAST represents a surface in which a change in fluvial style takes place. This
574 surface (or zone) of change could represent the expansion surface of Martinsen
575 et al. (1999) that can be correlated with the maximum regression surface. This
576 stratigraphic pattern reflects increasing accommodation space, with
577 pedogenesis mainly occurring during high-accommodation system tracts. At a
578 basinal scale, the vertical changes in the degree of development or maturity of
579 the paleosols observed within the early Cenozoic deposits of the eastern GSJB
580 (see Fig. 4) are consistent with the regional accommodation trends.

581 In the northern area of the GSJB, particularly in the Las Violetas
582 Formation, a strong volcanoclastic component is recorded; meanwhile, its lateral
583 equivalent, the Peñas Coloradas Formation, is predominately epiclastic in
584 composition (Raigemborn, 2006; 2008). The architectural features indicate
585 relatively low aggradation rate conditions and a relatively high volume of
586 sediment supply (low A/S ratio), which in the case of the Las Violetas
587 Formation, was mainly volcanoclastic (Raigemborn, 2008). This high sediment
588 supply of volcanoclastic material for the Las Violetas Formation was probably
589 provided by the erosion of the lower Paleocene basalts that crop out near to the
590 Estancia Las Violetas section, and which could act as a local source area, as
591 was mentioned by Foix et al. (2013). Volcanoclastic supply also increased during
592 the Río Chico Group–lower Sarmiento Formation deposition, accompanied by a
593 compositional change in the volcanoclastics, from basic to acid (Raigemborn,
594 2008; Raigemborn et al., 2018a). Raigemborn et al. (2018a and cited herein)
595 point out that volcanoclastic material of the Koluel-Kaike Formation generated at

596 the Pilcaniyeu Volcanic Belt and caldera field of this belt, 300–400 km to the
597 northwest of the analyzed sections.

598 Facies distribution and fluvial architecture of the Río Chico Group also
599 reflect spatial accommodation variability in the basin. Thick, amalgamated
600 coarse-grained intervals formed during low-accommodation conditions in the
601 basin margins (e.g., Estancia Las Violetas); meanwhile, more isolated, ribbon-
602 shaped sandy bodies are defined as lateral equivalents towards the west and
603 south of the basin. Foix et al. (2013, 2015) indicated that Puerto Visser locality,
604 a site between Estancia Las Violetas and Rocas Coloradas area (Fig. 1B),
605 would represent a break-point in the stratigraphic architecture of the unit at the
606 northeastern North Flank of the GSJB, separating two settings of variable
607 accommodation rates. Northwards Puerto Visser, the width/thick ratio of sandy
608 bodies and the channel/floodplain ratio increases; meanwhile, towards the
609 south, an increase in total thickness of the Río Chico Group and
610 accommodation is demonstrated by Foix et al. (2013, 2015). These authors
611 assumed that climate conditions were stable during times of the Río Chico
612 Group, and consequently, they discarded climate and sea-level changes as
613 controls over the fluvial architecture. Therefore, they infer that significant spatial
614 variations are due to the differential subsidence of the basin. At the same time,
615 Gianni et al. (2017) identified evidence of syntectonic deposition in the
616 middle/upper part of the Koluel-Kaike Formation (~ 44 Ma) in the eastern of the
617 San Bernardo Fold Belt, which is indicative of the occurrence of Eocene
618 intraplate tectonics in this area of the GSJB. However, we interpreted that the
619 overall horizontal disposition of the strata of the Río Chico Group, and the lack
620 of degradational features (i.e., incised valleys and terraces) in the study area,

621 indicate the occurrence of flat land surfaces and negligible tectonic activity
622 during the deposition of the unit, and that the system was mainly aggradational.

623

624 6. Final remarks and conclusions

625

626 Because changes in the relative proportion of channel and floodplain
627 deposits respond to changes in accommodation/sediment supply rate (A/S)
628 (e.g., Catuneanu, 2006; Beilinson et al., 2013; Foix et al., 2013, 2015; Di Celma
629 et al., 2015, among others), we were able to internally divide sequences into
630 low- and high-accommodation systems tract (i.e., LAST and HAST,
631 respectively) (Fig. 4). The LASTs defined in the Río Chico Group are typically
632 channel-dominated and formed on top of subaerial unconformities, suggesting
633 periods of low A/S ratio. The behavior of fluvial channels under these conditions
634 generated regional unconformities (sequence boundaries). Although some fine-
635 grained deposits of the floodplain can be developed during this stage, they have
636 a low probability of preservation, and consequently, only paleosols with a very
637 strong/strong degree of development can be formed.

638 The temporal resolution of the Río Chico Group at the west of the
639 eastern GSJB and the eastern of the San Bernardo Fold Belt (Clyde et al.,
640 2014; Krause et al., 2017) in combination with this stratigraphic sequential
641 analysis implies that at least one of the here identified stratigraphic
642 unconformities (SB3) might have formed during the optimum climatic of the
643 early Eocene (EECO, c. 53 to 51 Ma; Zachos et al., 2008), and that other two
644 might have formed during the greenhouse to icehouse transition (SB4 and

645 SB5). These three sequence boundaries span hundreds of thousands to
646 millions of years (10^5 – 10^6 yr; Bellosi, 2010b; Raigemborn et al., 2018a).

647 The integration of sedimentological and paleopedological analyses of the
648 four identified sequences into the Río Chico Group–lower Sarmiento Formation
649 in the eastern areas of the Golfo San Jorge Basin indicate that the interplay
650 between subsidence, base level, and climate-controlled fluvial/alluvial style and
651 landscape evolution of the units, as well as soil development. Volcaniclastic
652 supply also played a significant role, especially during the Eocene.

653

654 Acknowledgments

655

656 Financial and logistical support for these studies was provided by the
657 projects PIP 100523 of the CONICET and the PI+D N890 of the UNLP (to
658 MSR). The authors would like to thank L. Gómez Peral, L. Perez, S. Lizzoli, and
659 E. Melendi (CONICET-UNLP, Argentina) for their assistance during field trips to
660 the South Flank. The suggestions made by the reviewers, Dr G. Basilici and
661 one anonymous reviewer, and by the Editor Dr J.M. Paredes, greatly improved
662 the quality of this manuscript.

663

664 References

665

666 Amorosi, A., Bruno, L., Rossi, V., Severi, P., Hajdas, I., 2014. Paleosol
667 architecture of a late Quaternary basin-margin sequence and its
668 implications for highresolution, non-marine sequence stratigraphy: Global
669 and Planetary Change, 112, 12–25.

- 670 Amorosi, A., Bruno, L., Cleveland, D., Morelli, A., Hong, W., 2017. Paleosols
671 and associated channel-belt sand bodies from a continuously subsiding
672 late Quaternary system (Po Basin, Italy): New insights into continental
673 sequence stratigraphy. *Geological Society of America Bulletin*, 129, 449–
674 463.
- 675
676 Andreis, R.R., Mazzoni, M.M., Spalletti, L.A., 1975. Estudio estratigráfico y
677 paleoambiental de las sedimentitas terciarias entre Pico Salamanca y
678 Bahía Bustamante, provincia del Chubut, República Argentina. *Rev. Asoc.*
679 *Geol. Argent.*, 30, 85–103.
- 680 Ashley, G., Deocampo, D.M., Kahmann-Robinson, J.A., Driese, S., 2013.
681 Groundwater-fed wetland sediments and paleosols: it's all about water
682 table. In: Driese, S.G., Nordt, L.C. (Eds.), *New Frontiers in Paleopedology*
683 *and Terrestrial Paleoclimatology: Paleosols and Soil Surface Analogue*
684 *Systems*, vol. 104. Society for Sedimentary Geology, Special Publication,
685 pp. 47–61.
- 686 Beilinson, E., Veiga, G.D., Spalletti, L.A., 2013. High-resolution sequence
687 stratigraphy and continental environmental evolution: an example from
688 east-central Argentina. *Sedimentary Geology*, 296, 21–35.
- 689 Bellosi, E.S., 2010a. Loessic and fluvial sedimentation of Sarmiento Formation
690 pyroclastics in the Middle Cenozoic of central Patagonia. In: Madden,
691 R.H., Carlini, A.A., Vucetich, M.G., Kay, R.F. (Eds.). *The Paleontology of*
692 *Gran Barranca: Evolution and Environmental Change through the Middle*
693 *Cenozoic of Patagonia*. Cambridge University Press, Cambridge, UK, pp.
694 278–292.

- 695 Bellosi, E.S., 2010b. Physical stratigraphy of the Sarmiento Formation (Middle
696 Eocene–Lower Miocene) at Gran Barranca, central Patagonia. In:
697 Madden, R.H., Carlini, A.A., Vucetich, M.G., Kay, R.F. (Eds.), *The*
698 *Paleontology of Gran Barranca: Evolution and Environmental Change*
699 *Through the Middle Cenozoic of Patagonia*. Cambridge University Press,
700 Cambridge, UK, pp. 19–31.
- 701 Bellosi, E.S., González, M.G., 2010. Paleosols of the middle Cenozoic
702 Sarmiento Formation, central Patagonia. In: Madden, R.H., Carlini, A.A.,
703 Vucetich, M.G., Kay, R. (Eds.), *The Paleontology of Gran Barranca:*
704 *Evolution and Environmental Change Through the Middle Cenozoic of*
705 *Patagonia*. Cambridge University Press, Cambridge, UK, pp. 293–305.
- 706 Bown, T.M., Kraus, M.J., 1987. Integration of channel and floodplain suites in
707 aggrading fluvial systems. 1. Developmental sequence and lateral
708 relations of lower Eocene alluvial paleosols, Willwood Formation, Bighorn
709 Basin, Wyoming: *Journal of Sedimentary Petrology*, 57, 587–601.
- 710 Bridge, J.S., 2003. *Rivers and Floodplains: Forms, Processes, and Sedimentary*
711 *Record*. Blackwell Science Publishing, Oxford, 491 pp..
- 712 Catuneanu, O., 2006. *Principles of Sequence Stratigraphy*. Elsevier, 375 pp.
- 713 Clyde, W.C., Wilf, P., Iglesias, A., Slingerland, R.L., Barnum, T., Bijl, P.K.,
714 Bralower, T.J., Brinkhuis, H., Comer, E.E., Huber, B.T., Ibañez-Mejía, M.,
715 Jicha, B.R., Krause, J.M., Schueth, J.D., Singer, B.S., Raigemborn, M.S.,
716 Schmitz, M.D., Sluijs, A., Zamaloa, M. del C., 2014. New age constraints
717 for the Salamanca Formation and lower Río Chico Group in the western
718 San Jorge Basin, Patagonia, Argentina: Implications for K/Pg extinction

- 719 recovery and land mammal age correlations. Geological Society of
720 America Bulletin doi:10.1130/B30915.1, 1–18.
- 721 Comer, E.E., Slingerland, R.L., Krause, J.M., Iglesias, A., Clyde, W.C.,
722 Raigemborn, M.S., Wilf, P., 2015. Sedimentary facies and depositional
723 environments of diverse early Paleocene floras, north-central San Jorge
724 Basin, Patagonia, Argentina. *Palaios* 30, 553–573.
725 <http://dx.doi.org/10.2110/palo.2014.064>.
- 726 Dahle, K., Flesja, K., Talbot, M.R., Dreyer, T., 1997. Correlation of fluvial
727 deposits by the use of Sm–Nd isotope analysis and mapping of
728 sedimentary architecture in the Escanilla Formation (Ainsa Basin, Spain)
729 and the Staffjord Formation (Norwegian North Sea). Abstracts, Sixth
730 International Conference on Fluvial Sedimentology, Cape Town, South
731 Africa, p. 46.
- 732 Demko, T.M., Currie, B.S., Nicoll, K.A., 2004. Regional paleoclimatic and
733 stratigraphic implications of paleosols and fluvial/overbank architecture in
734 the Morrison Formation (Upper Jurassic), Western Interior, USA:
735 *Sedimentary Geology*, 167, 115–135.
- 736 Di Celma, C., Pieruccini, P., Farabollini, P., 2015. Major controls on
737 architecture, sequence stratigraphy and paleosols of middle Pleistocene
738 continental sediments ("Qc Unit"), eastern central Italy. *Quaternary*
739 *Research* 83, 565–581.
- 740 Dunn, R.; Madden, R.; Kohn, M.; Schmitz, M.; Strömberg, C.; Carlini, A.; Ré, G.;
741 Crowley, J., 2013. A new chronology for middle Eocene–early Miocene
742 South American Land Mammal Ages. *Geological Society of America*
743 *Bulletin* 125, 539–555.

- 744 Feruglio, E., 1949. Descripción geológica de la Patagonia I, II, III. Dirección
745 General de Yacimientos Petrolíferos Fiscales. Buenos Aires, Argentina, p.
746 750.
- 747 Foix, N., Paredes, J.M., Giacosa, R.E., 2008. Paleo-earthquakes in passive
748 margin settings, an example from the Paleocene of the Golfo San Jorge
749 Basin, Argentina. *Sedimentary Geology* 205, 67–75.
- 750 Foix, N., Paredes, J.M., Giacosa, R.E., 2012. Upper Cretaceous–Paleocene
751 normal reactivation phase in the Golfo San Jorge Basin (Argentina):
752 growth-fault models, paleoseismicity and paleostress analysis. *Journal of*
753 *South American Earth Science* 33, 110–118.
- 754 Foix, N., Paredes, J.M., Giacosa, R.E., 2013. Fluvial architecture variations
755 linked to changes in accommodation space: Río Chico Formation (Late
756 Paleocene), Golfo San Jorge basin, Argentina. *Sedimentary Geology*, 394,
757 342–355.
- 758 Foix, N., Paredes, J.M., Giacosa, R.E., Allard, J.O., 2015. Arquitectura
759 estratigráfica del Paleoceno en el flanco norte de la Cuenca Del Golfo San
760 Jorge. *Patagon. Cent. Rev. Asoc. Geol. Arg.*, 72, 96–106.
- 761 Figari, E., Strelkov, E., Laffite, G., Cid de la Paz, M., Courtade, S., Celaya, J.,
762 Vottero, A., Lafourcade, S., Martinez, R., Villar, H., 1999. Los sistemas
763 petroleros de la Cuenca del Golfo San Jorge: Síntesis estructural,
764 estratigráfica y geoquímica. 4° Congreso de Exploración y Desarrollo de
765 Hidrocarburos. *Actas*, Buenos Aires, pp. 197–237.
- 766 Fitzgerald, M.G., Mitchum, R.M., Uliana, M.A., Biddle, K.T., 1990. Evolution of
767 the San Jorge Basin, Argentina. *AAPG Bulletin*, 74, 879–920.

- 768 Giampaoli, P., 2015. Caracterización de sistemas de fallas extensionales
769 utilizando perfiles y mapas de desplazamiento: ejemplos del Cretácico de
770 la cuenca del Golfo San Jorge. *Rev. Asoc. Geol. Argent.* 72, 111–123.
- 771 Gianni, G.M., Echaurren, A., Folguera, A., Likerman, J., Encinas, A., García,
772 H.P.A., Dal Molin, C., Valencia, V.A., 2017. Cenozoic intraplate tectonics
773 in Central Patagonia: record of main Andean phases in a weak upper
774 plate. *Tectonophysics* 721, 151–166.
- 775 Gómez Peral, L., Raigemborn, M.S., Richiano, S., Arruy, M.J., Odino-Barreto,
776 A.L., Pérez, L.M., Sial, A., Ferreyra, C., 2019. Decoding depositional and
777 diagenetic conditions of the mid-Cenozoic Puesto del Museo Formation,
778 southern Golfo San Jorge Basin, Patagonia, Argentina. *Journal of South
779 American Earth Sciences*, 96. DOI:
780 <https://doi.org/10.1016/j.jsames.2019.102356>
- 781 Hechem, J.J., Strelkov, E.E., 2002. Secuencia sedimentaria mesozoica del
782 Golfo San Jorge. In: Haller, J.M. (Ed.), *Geología y Recursos Naturales de
783 Santa Cruz. Relatorio del XV Congreso Geológico Argentino. Asociación
784 Geológica Argentina, Buenos aires*, pp. 129–147.
- 785 Homocv, J.F., Conforto, G.A., Lafourcade, P.A., Chelotti, L.A., 1995. Fold belt in
786 the San Jorge Basin, Argentine: an example of tectonic inversion. In:
787 Buchanan, J.G., Buchanan, P.G. (Eds.), *Basin Inversion. Special
788 Publication, Geological Society of London*, pp. 235–248.
- 789 Iglesias, A., 2007. Estudio paleobotánico, paleoecológico y paleoambiental en
790 secuencias de la Formación Salamanca, del Paleoceno Inferior en el sur
791 de la Provincia de Chubut, Patagonia, Argentina [Ph.D. thesis,

- 792 unpublished]: La Plata, Argentina, Universidad Nacional de La Plata, 244
793 pp.
- 794 Iglesias, A., Wilf, P., Johnson, K.R., Zamuner, A.B., Cúneo, N.R., Matheos,
795 S.D., and Singer, B.S., 2007. A Paleocene lowland macroflora from
796 Patagonia reveals significantly greater richness than North American
797 analogs: *Geology* 35, 947–950.
- 798 Kraus, M., 1999. Paleosols in clastic sedimentary rocks. *Earth Sciences*
799 *Reviews* 47, 41–70.
- 800 Krause, J.M., Bellosi, E.S., Raigemborn, M.S., 2010a. Lateritized tephric
801 palaeosols from Central Patagonia, Argentina: a southern high-latitude
802 archive of Palaeogene global greenhouse conditions. *Sedimentology* 57,
803 1721–1749.
- 804 Krause, J.M., White, T.S., Raigemborn M.S., Bellosi, E.S., 2010b. Palaeosols of
805 the Peñas Coloradas Formation: warm and humid conditions in the Late
806 Palaeocene of Central Patagonia. 18th International Sedimentological
807 Congress, Mendoza, Argentina. Abstracts Volume, 516.
- 808 Krause, J.M., Clyde, W.C., Ibañez-Mejía, M., Schmitz, M.D., Barnum, T.,
809 Bellosi, E., Wilf, P., 2017. New age constraints for early Paleogene strata
810 of central Patagonia, Argentina: implications for the timing of South
811 American land mammal ages. *Geol. Soc. Am. Bull.*
812 <https://doi.org/10.1130/B31561.1>.
- 813 Krause, J.M., and Piña, C.I., 2012, Reptilian coprolites in the Eocene of central
814 Patagonia, Argentina: *Journal of Paleontology* 86 (3), 527–538, doi: 10
815 .1666 /11-075 .1.

- 816 Legarreta, L., Uliana, M.A., 1994. Asociaciones de fósiles y hiatos en el
817 Supracretácico-Neógeno de la Patagonia: Una perspectiva estratigráfico-
818 secuencial. *Ameghiniana*, 31, 257–281.
- 819 Legarreta, L., Uliana, M.A., Torres, M., 1990. Secuencias deposicionales
820 cenozoicas de Patagonia Central: sus relaciones con las asociaciones de
821 mamíferos terrestres y episodios marinos epicontinentales. 3° Simposio
822 del Terciario de Chile, Actas. Sociedad Geológica de Chile, Concepción,
823 pp. 135–176.
- 824 Lizzoli, S., Martegani, L., Raigemborn, M.S., (2018). Procesos pedogenéticos
825 en una sucesión del Paleógeno de Patagonia a partir de la aplicación de
826 técnicas micromorfológicas. XVI Reunión Argentina de Sedimentología.
827 General Roca, Actas, 28.
- 828 Malumián, N., Ardolino, A.A., Franchi, M., Remesal, M., Salini, F., 1999. La
829 sedimentación y el volcanismo terciarios en la Patagonia Extraandina. In:
830 Caminos, R. (Ed.), *Geología Argentina, Anales*, vol. 29 (18). Instituto de
831 Geología y Recursos Minerales, pp. 557–612.
- 832 Malumián, N., Nañez, C., 2011. The Late Cretaceous–Cenozoic transgressions
833 in Patagonia and the Fuegian Andes: foraminifera, palaeoecology, and
834 palaeogeography. *Biol. J. of the Linn. Soc.*, 103, 269–288.
- 835 Martínez, G.A., 1992. Paleoambiente de la Formación Salamanca en La Pampa
836 María Santísima, Departamento Sarmiento. Prov. Chubut. *Rev. Asoc.*
837 *Geol. Argent.*, 47, 293–303.
- 838 Matheos, S.D., Brea, M., Ganuza, D., Zamuner, A., 2001. Sedimentología y
839 paleoecología del Terciario Inferior en el sur de la Provincia del Chubut,
840 República Argentina. *AAS Rev.*, 8, 93–104.

- 841 Marriott, S., Wright, V., 1993. Paleosols as indicators of geomorphic stability in
842 two Old Red Sandstone alluvial suites, South Wales. *Journal of the*
843 *Geological Society of London* 150, 1109–1120.
- 844 McCarthy, P.J., Plint, A.G., 2013. A pedostratigraphic approach to nonmarine
845 sequence stratigraphy: a three-dimensional paleosol-landscape model
846 from the Cretaceous (Cenomanian) Dunvegan Formation, Alberta and
847 British Columbia, Canada. In: Driese, S.G., Nordt, L.C. (Eds.). *New*
848 *frontiers in Paleopedology and terrestrial paleoclimatology. Paleosols and*
849 *soil surface analog systems. SEPM SP. 104*, pp. 159–177.
- 850 Miall, A.D., 1996. *The Geology of Fluvial Deposits: Sedimentary Facies, Basin*
851 *Analysis and Petroleum Geology*. Springer-Verlag, Berlin, 582 pp.
- 852 Munsell Soil Color Book, 2013. Grand Rapids: Munsell Color. X-Rite, USA
853 2013.
- 854 Opluštil, S., Lojka, R., Rosenau, N., Strnad, L., Sýkorová, I., 2015. Middle
855 Moscovian climate of eastern equatorial Pangea recorded in paleosols
856 and fluvial architecture. *Palaeogeography, Palaeoclimatology,*
857 *Palaeoecology* 440, 328–352.
- 858 Paredes, J.M., Foix, N., Colombo Piñol, F., Nillni, A., Allard, J.O., Marquillas,
859 R.A., 2007. Volcanic and climatic control on fluvial style in a high-energy
860 system: the Lower Cretaceous Matasiente Formation, Golfo San Jorge
861 Basin, Argentina. *Sedimentary Geology* 202, 96–123.
- 862 Paredes, J., Foix, N., Guerstein, R., Guler, M.V., Irigoyen, M., Moscoso, P.,
863 Giordano, S., 2015. A late Eocene-early Oligocene transgressive event in
864 the Golfo San Jorge basin: Palynological results and stratigraphic
865 implications. *Journal of South American Earth Sciences* 63, 293–309.

- 866 Paredes, J.M., Aguiar, M., Ansa, A., Giordano, S.R., Ledesma, M., Tejada, S.,
867 2018. Inherited discontinuities and fault kinematics of a multiphase, non-
868 colinear extensional setting: subsurface observations from the south Flank
869 of the Golfo san Jorge basin, Patagonia. *Journal of South American Earth*
870 *Sciences*, 81, 87–107.
- 871 Raigemborn, M.S., 2006. Análisis composicional y procedencia de la Formación
872 Peñas Coloradas, Grupo Río Chico (Paleoceno superior-Eoceno?), en la
873 región oriental de la Cuenca del Golfo San Jorge, Chubut, Argentina. *Latin*
874 *American Journal of Sedimentology and Basin Analysis* 13, 119–133.
- 875 Raigemborn, M.S., 2008. Estudio Estratigráfico, Sedimentológico y
876 Composicional de las Sedimentitas del Terciario Inferior (Grupo Río
877 Chico) en el Sector Sudoriental del Chubut Extraandino [Ph.D.
878 thesis]: La Plata, Argentina, Universidad Nacional de La Plata, 352 p.
- 879 Raigemborn, M., Brea, M., Zucol, A., Matheos, S., 2009a. Early Paleogene
880 climate at mid latitude in South America: mineralogical and paleobotanical
881 proxies from continental sequences in Golfo San Jorge basin (Patagonia,
882 Argentina). *Geologica Acta*, 7, 125–146.
- 883 Raigemborn, M.S., Krause, J.M., Matheos, S., 2009b. Continental
884 sedimentation of the Las Flores Formation (Early Palaeogene) in Golfo
885 San Jorge Basin (Patagonia, Argentina). 27th Meeting of Sedimentology,
886 Alghero, Italia. Libro de Abstracts, p. 650.
- 887 Raigemborn, M.S., Krause, J.M., Bellosi, E., Matheos, S.D., 2010. Redefinición
888 estratigráfica del Grupo Río Chico (Paleógeno inferior), en el norte de la
889 cuenca del Golfo San Jorge, Chubut, Argentina. *Revista de la Asociación*
890 *Geológica Argentina* 67, 239–256.

- 891 Raigemborn, M.S., Gómez-Peral, L., Krause, J.M., Matheos, S.D., 2014.
892 Controls on clay mineral assemblages in an Early Paleogene nonmarine
893 succession: Implications for the volcanic and paleoclimatic record of extra-
894 Andean Patagonia, Argentina: *Journal of South American Earth Sciences*
895 52, 1–23.
- 896 Raigemborn, M.S., Beilinson, E., Krause, J.M., Varela, A.N., Bellosi, E.,
897 Matheos, S., Sosa, N., 2018a. Paleolandscape reconstruction and
898 interplay of controlling factors of an Eocene pedogenically-modified distal
899 volcanoclastic succession in Patagonia. *Journal of South American Earth*
900 *Sciences* 86, 475-496.
- 901 Raigemborn, M.S., Iglesias, A., Gómez Peral, L., Brea, M., Arrouy, J.,
902 Stromberg, C., Beilinson, E., Pérez, L., Matheos, S., 2018b. Una mirada
903 multidisciplinaria para estimar el paleoclima del Paleógeno inferior de
904 Patagonia (Argentina). XVI Reunión Argentina de Sedimentología.
905 General Roca, Actas, p. 167.
- 906 Ré, G.; Bellosi, E.S.; Heizler, M.; Vilas, J.; Madden, R.; Carlini, A.; Kay, R.;
907 Vucetich, M.G. 2010. Geochronology for the Sarmiento Formation at Gran
908 Barranca. In: Madden, R., Carlini, A., Vucetich, M., Kay, R. (Eds.). *The*
909 *Paleontology of Gran Barranca: evolution and environmental change*
910 *through the Middle Cenozoic of Patagonia*. Cambridge University Press,
911 Cambridge, pp. 46–59.
- 912 Retallack, G., 1994. A pedotype approach to latest Cretaceous and earliest
913 Tertiary paleosols in eastern Montana. *Geol. Soc. Am. Bull.* 106, 1377–
914 1397.

- 915 Retallack, G.J., 2001. *Soils of the past*, 2nd ed. Blackwell Science Ltd., Oxford,
916 404 pp.
- 917 Ruiz, D.P., Brea, M., Raigemborn, M.S., Matheos, S.D., 2017. Conifer fossil
918 woods from the Salamanca Formation (early Paleocene) from the Estancia
919 Las Violetas, Central Patagonia, Argentina: paleoenvironmental
920 implications. *Journal of South American Earth Sciences*, 76, 427–445.
921 DOI: <http://dx.doi.org/10.1016/j.jsames.2017.04.006>.
- 922 Ruiz, D.P., Raigemborn, M.S., Brea, M., Pujana, R.R., 2020. Paleocene Las
923 Violetas Fossil Forest: wood anatomy and paleoclimatology. *Journal of*
924 *South American Earth Sciences*, 98. DOI:
925 <https://doi.org/10.1016/j.jsames.2019.102414>
- 926 Shanley, K.W., McCabe, P.J., 1994. Perspectives on the sequence stratigraphy
927 of continental strata: *American Association of Petroleum Geologists*
928 *Bulletin*, 78, 544–568.
- 929 Soil Survey Staff, 1999. *Soil Taxonomy, a Basic System for Making and*
930 *Interpreting Soil Surveys*. United States Department of Agriculture,
931 Handbook, Washington, pp. 436.
- 932 Soil Survey Staff, 1975. *Soil Taxonomy*. United States Department of
933 Agriculture,
934 Washington, DC.
- 935 Soil Survey Staff, 1998. *Key to Soil Taxonomy*. 8th edn. United States
936 Department of Agriculture, Natural Resources Conservation Service,
937 Washington, DC.

- 938 Varela, A.N., Veiga, G.D., Poiré, D.G., 2012. Sequence stratigraphic analysis of
939 Cenomanian greenhouse palaeosols: a case study from southern
940 Patagonia, Argentina. *Sedimentary Geology* 271 (272), 67–82.
- 941 Wright, V.P., Marriott, S.B., 1993. The sequence stratigraphy of fluvial
942 depositional systems: The role of floodplain sediment storage:
943 *Sedimentary Geology* 86, 203–210.
- 944 Woodburne, M.O., Goin, F.J., Raigemborn, M.S., Heizler, M., Gelfo, J.N.,
945 Oliveira, E.V., 2014. Revised timing of the South American early
946 Paleogene Land Mammal Ages. *Journal of South American Earth
947 Sciences* 54, 109–119.
- 948 Zachos, J.C., Pagani, M., Sloan, L., Thomas, E., Billups, K., 2001. Trends,
949 rhythms, and aberrations in global climate 65 Ma to present: *Science* 292,
950 686–693, doi:10.1126 /science.1059412.
- 951 Zachos, J.C., Dickens, G.R., Zeebe, R.E., 2008. An early Cenozoic perspective
952 on greenhouse warming and carbon-cycle dynamics. *Nature* 451, 279–
953 283.
- 954 Zucol, A.F., Krause, J.M., Brea, M., Raigemborn, M.S., Matheos, S., 2018.
955 Emergence of grassy habitats during the greenhouse–icehouse Systems
956 transition in the Middle Eocene of Central Patagonia. *Ameghiniana* 55,
957 451–482. DOI:10.5710/AMGH.12.03.2018.3152.

958

959 **TABLES AND FIGURES**

960

961 **Table 1.** Summary chart of the facies associations (FA) identified in the Río
962 Chico Group.

963

964 **Table 2.** Summary of the most distinctive pedogenic features within the
965 paleosols of the Río Chico Group and lower Sarmiento Formation.

966

967 **Figure 1.** Map showing position, boundaries, and internal division of the Golfo
968 San Jorge Basin (A), and location of the localities included in this paper (B). The
969 dotted line in 1B marks the boundary between the Eastern Sector of the basin
970 and the San Bernardo Fold Belt.

971

972 **Figure 2.** Stratigraphic chart of the study area (eastern of the Golfo San Jorge
973 Basin). It extends through continental (white) and marine (gray and black)
974 successions from the early Paleocene to the late Eocene. The vertical shading
975 indicates a hiatus. Ages for the Salamanca Formation come from Clyde et al.
976 (2014), ages for the Río Chico Group are based on Krause et al. (2017), and
977 ages for the lower Sarmiento Formation are following Ré et al. (2010) and Dunn
978 et al. (2013).

979

980 **Figure 3.** Representative simplified measured sedimentary sections including
981 facies associations (FA), paleosol types, fluvial styles, and lithostratigraphic
982 units of the Eastern Golfo San Jorge Basin (modified from Raigemborn et al.,
983 2010, 2014, 2018a and b). Facies association color bar refer to the
984 predominantly facies association in such part of the profiles. Abbreviations: SF:
985 Salamanca Formation, BV: Banco Verde, BNI: Banco Negro Inferior, LVF: Las
986 Violetas Formation, PCF: Peñas Coloradas Formation, LFF: Las Flores
987 Formation, KKF: Koluel-Kaike Formation, SMF: Sarmiento Formation, CHF:

988 Chenque Formation, HF: Huemul Formation, DFD: Distal floodplain-dominated,
989 DEDFS: Distal eolian-dominated fluvial system.

990

991 **Figure 4.** Schematic diagram illustrating systems tract development during the
992 middle Paleocene–middle Eocene in the GSJB. Spatial variations in fluvial
993 architecture and paleosol development between the North Flank and the South
994 Flank are also depicted, as well as the correlation between the lithostratigraphic
995 units and the sequences here-by proposed. In the references box: HAST; high-
996 accommodation systems tract; LAST; low-accommodation systems tract; SB:
997 sequence boundary.

998

999 **Figure 5.** Representative outcrops of the Eastern Golfo San Jorge Basin
1000 showing different systems tracts (LAST and HAST) and sequence boundaries
1001 (SB). A: SB1 eroded upper deposits of the Salamanca Formation (SF), followed
1002 by the LAST1 and the HAST1 (LVF: Las Violetas Formation) at Estancia Las
1003 Violetas. The arrow marks the beginning of the HAST1, and the thin white line
1004 signals the contact with the Chenque Formation. B: SB1 developed over the
1005 upper deposits of the Salamanca Formation (SF) following by the LAST1 and
1006 the HAST1 (PCF: Peñas Coloradas Formation) at Cerro Abigarrado area. The
1007 arrow marks the beginning of the HAST1. The bar for scale is equivalent to 6 m.
1008 C: Irregular and erosional surface (SB2) separating the upper deposits of the
1009 Salamanca Formation (SF) from the overlying LAST2 and HST2 pedogenically
1010 modified of the Las Flores Formation (LFF), which are followed (SB3) by the
1011 pedogenically modified LAST3-HAST3 deposits of the upper Las Flores
1012 Formation and Koluel-Kaike Formation (KKF) at Laguna Manantiales. The gray

1013 arrow indicated the position of the very strongly developed paleosols that
1014 defined the position of the SB3, and the thin white line indicates the contact with
1015 overlying late Eocene basalts. The person as scale in the circle is ~1.60 m
1016 height. D: Erosive and irregular surface (SB2) separating HAST1 deposits of the
1017 Peñas Coloradas Formation (PCF) from the LAST2 deposits of the Las Flores
1018 Formation (LFF) at Rocas Coloradas area. The bar for scale is equivalent to 10
1019 m. E: Highly irregular and erosive surface (SB2) between the HAST1 (PCF:
1020 Peñas Coloradas Formation) and the LAST2 (LFF: Las Flores Formation) at
1021 Las Flores area. The person as scale, in the upper-left corner, is ~1.80 m
1022 height. F: HAST2 deposits of the Las Flores Formation (LFF) with very weak to
1023 weak developed paleosols and pedogenically modified lower Koluel-Kaike
1024 Formation (KKF), LAST3–HAST3 deposits of the middle-upper KKF
1025 represented by strongly-developed stacking paleosols that upwards changes to
1026 weakly developed ones, and the Sequence Boundary 3 (SB3) at the top of
1027 laterite-like paleosols (lower KKF) at Las Flores area. SMF: Sarmiento
1028 Formation. The bar for scale is equivalent to ~50 m.

1029

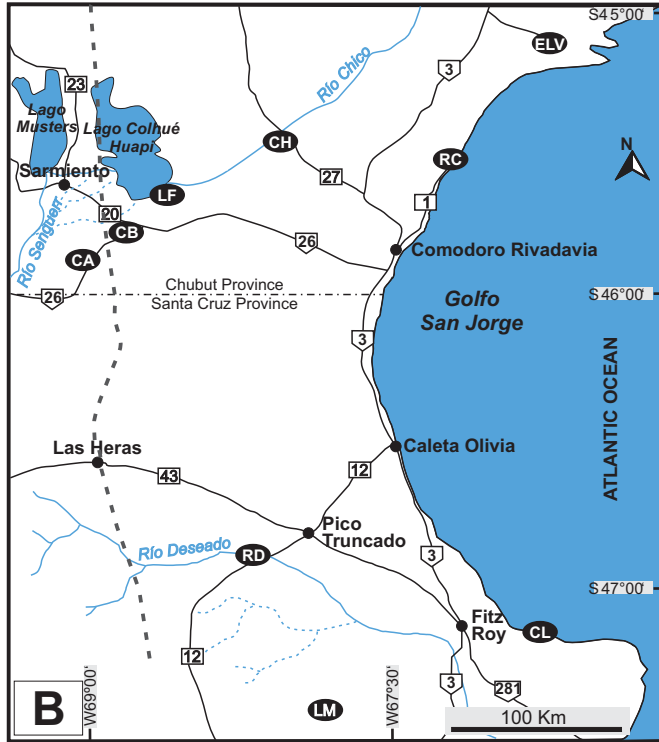
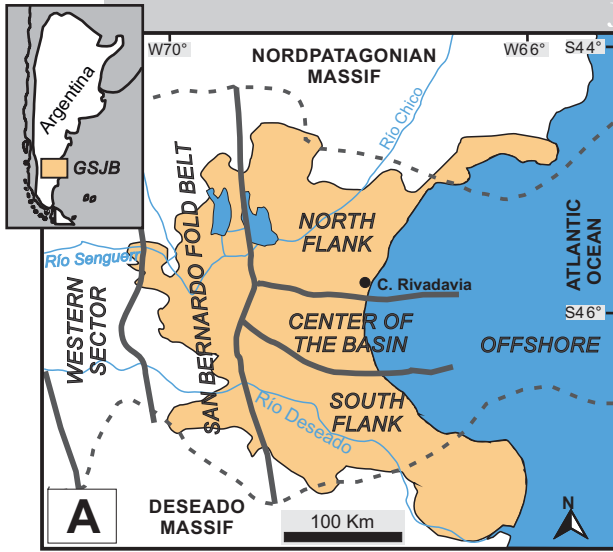
1030 **Figure 6.** Characteristic paleosol types, considering their degree of
1031 development, at the Eastern Golfo San Jorge Basin. A: Stacking of weakly to
1032 strong developed paleosols (Inceptisol-like and Alfisol-like paleosols) in the
1033 HAST 1 (Las Violetas Formation) at Estancia Las Violetas. B: Very weakly
1034 developed paleosol (Entisol-like) in the HAST1 (Peñas Coloradas Formation) at
1035 Rocas Coloradas area. C: Paleosol with weak degree of development
1036 (Inceptisol-like) at HAST2 (Las Flores Formation) at Las Flores area. D: Very
1037 strongly developed paleosols at the middle-upper Las Flores Formation (LFF)

1038 that defined the Sequence Boundary 3 (SB3) at Cerro Blanco. SB4 is at the top
1039 of very strongly developed paleosols, signed with an arrow at the lower Koluel-
1040 Kaike Formation (KKF). Persons as scale in the circle are ~1.80 and 1.60 m
1041 height, respectively. E: Strongly developed paleosols (Ultisol-like) in the HAST2
1042 (Las Flores Formation) at Laguna Manantiales. F: Very strongly developed
1043 paleosols (Plinthite-like) of the Sequence Boundary 4 (Koluel-Kaike Formation)
1044 at the Río Deseado area. The person as scale is ~1.70 m height.

1045

1046

1047

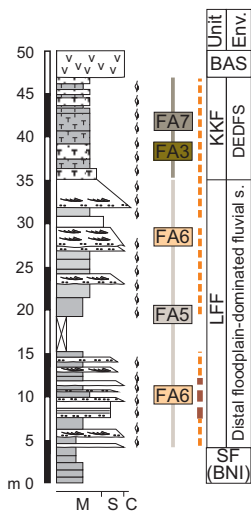


References

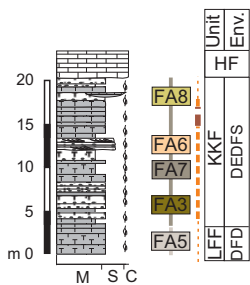
- | | |
|----------------------------------|--|
| ELV Estancia Las Violetas | CA Cerro Abigarrado area |
| RC Rocas Coloradas area | RD Río Deseado area |
| CH Cañadón Hondo area | CL Cañadón Lobo |
| LF Las Flores area | LM Laguna Manantiales |
| CB Cerro Blanco | 3 12 National and Provincial roads |

SW

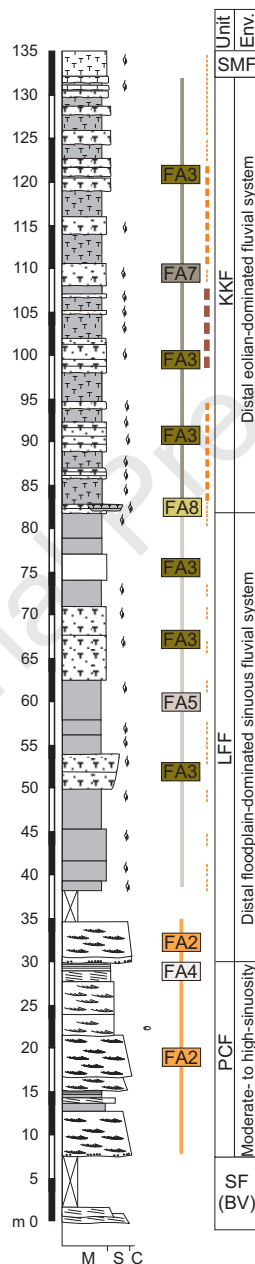
LAGUNA MANANTIALES



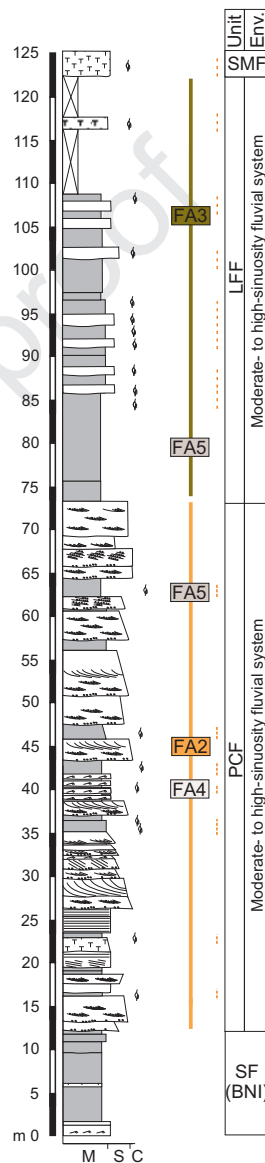
RÍO DESEADO AREA



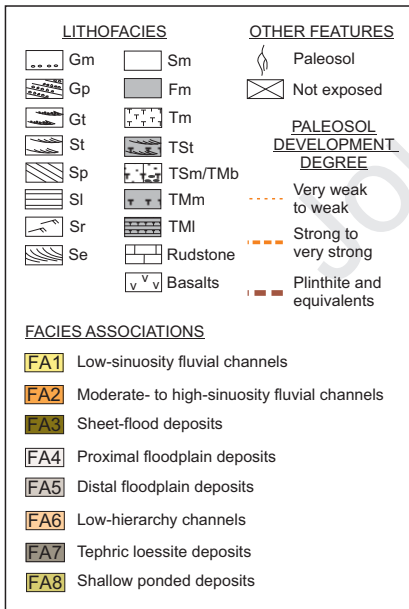
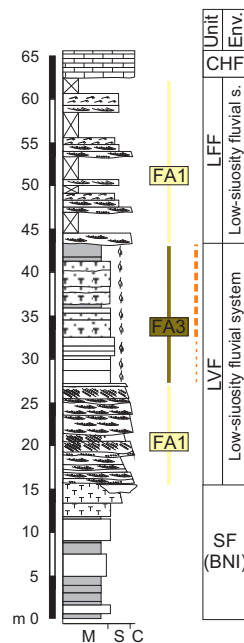
LAS FLORES AREA



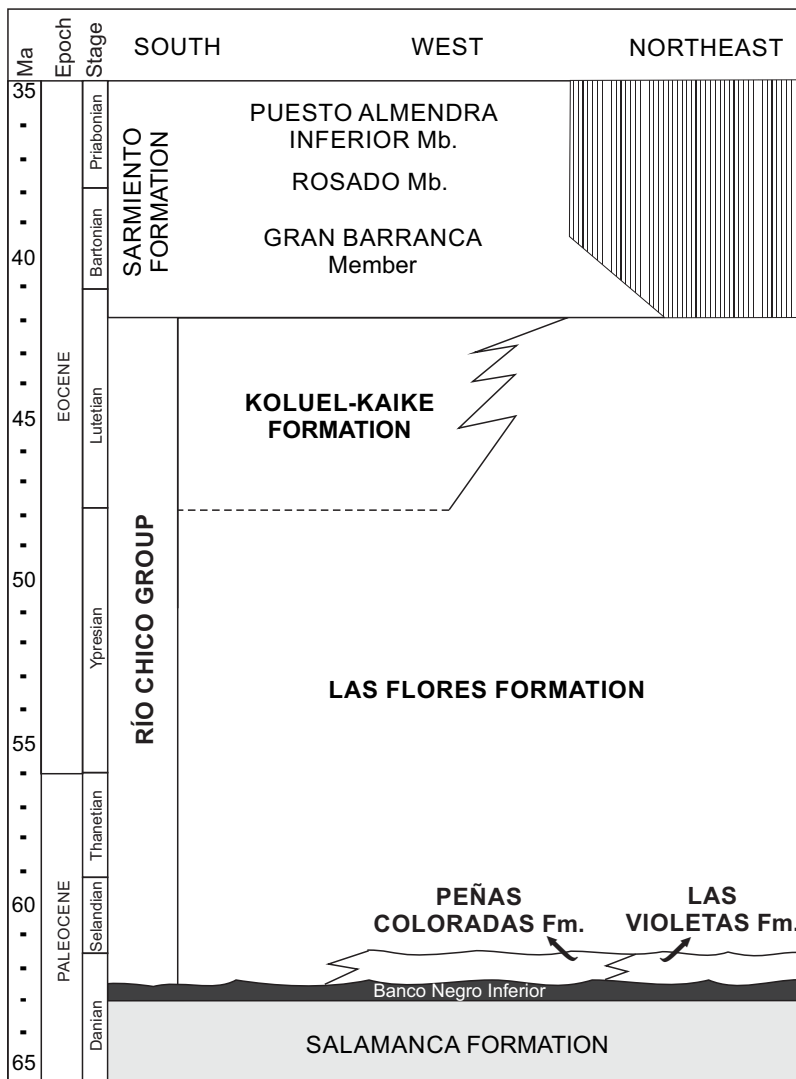
ROCAS COLORADAS AREA

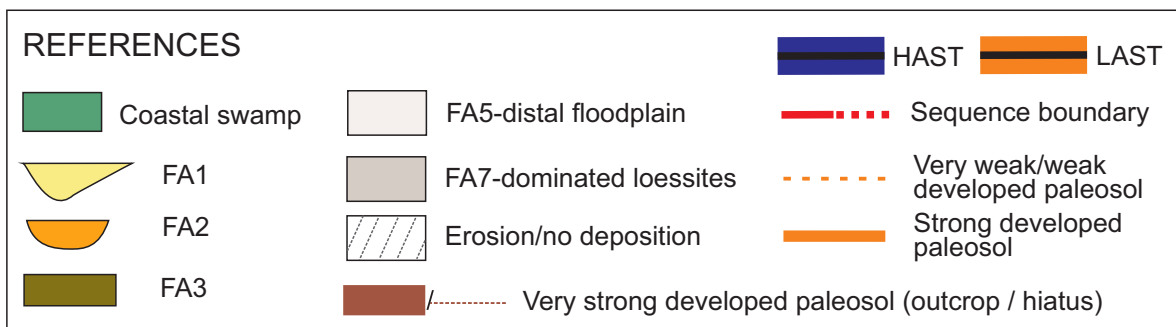
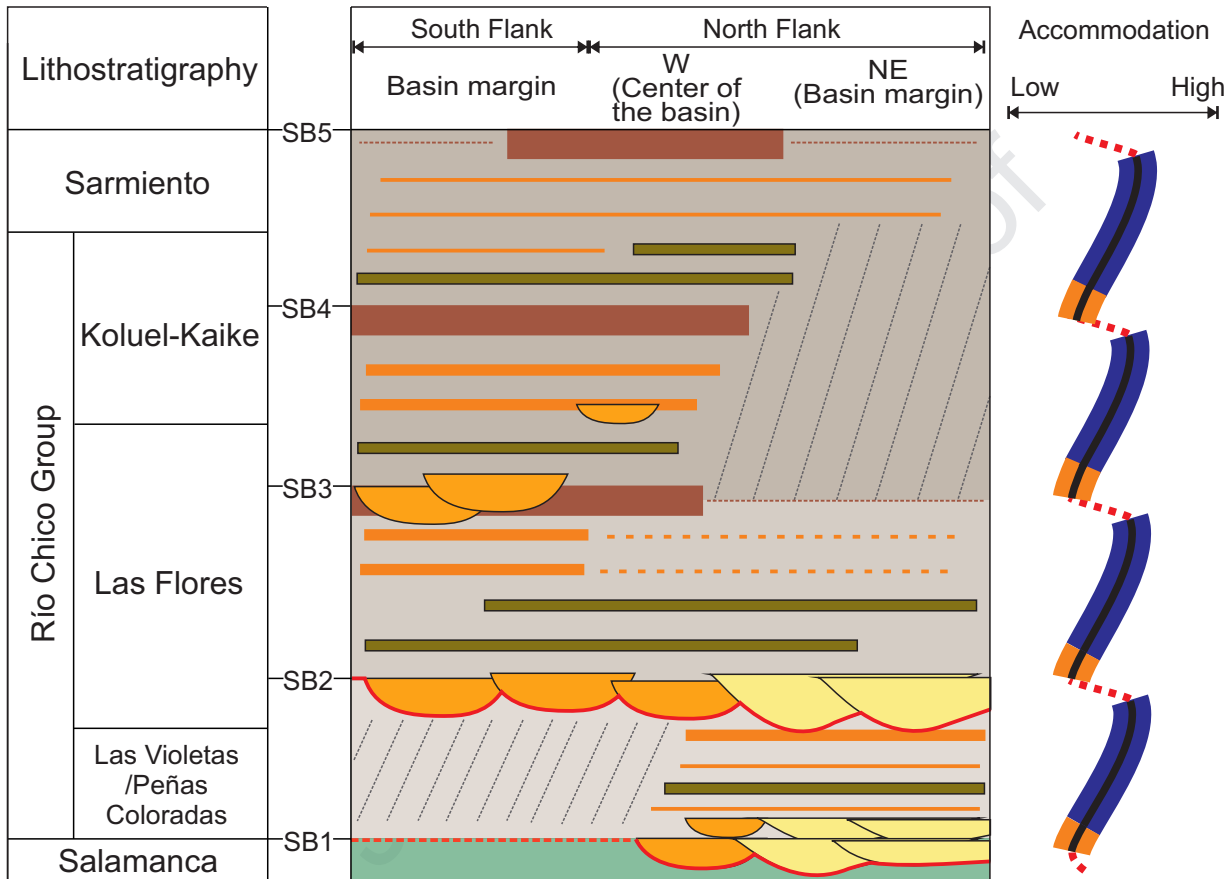


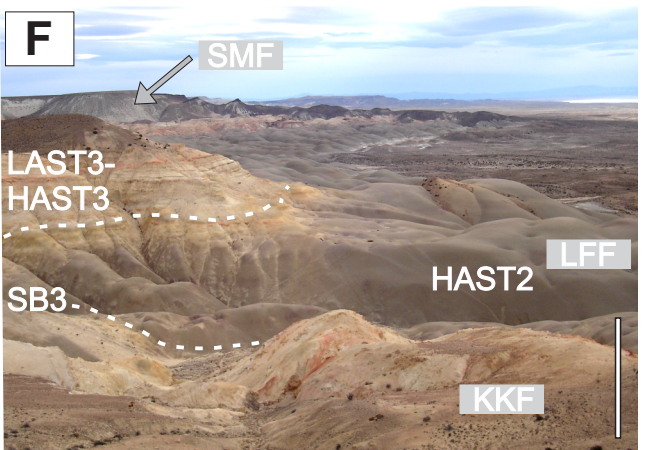
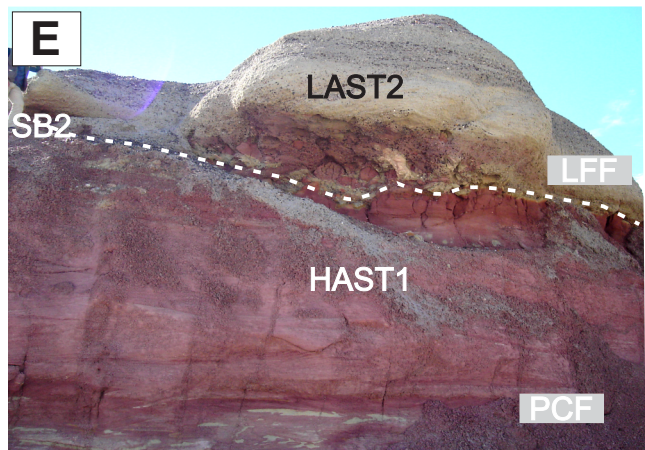
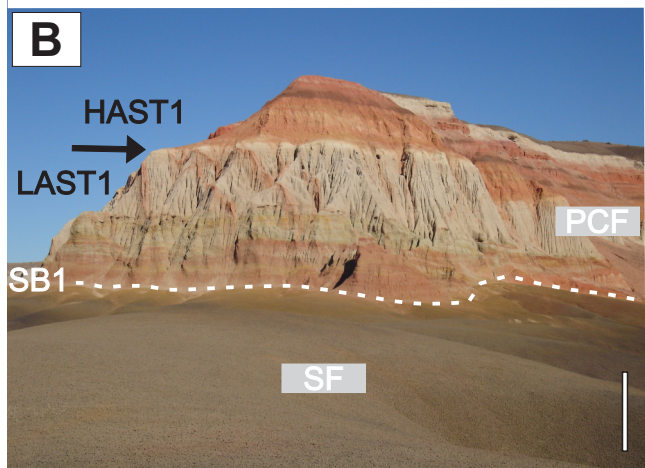
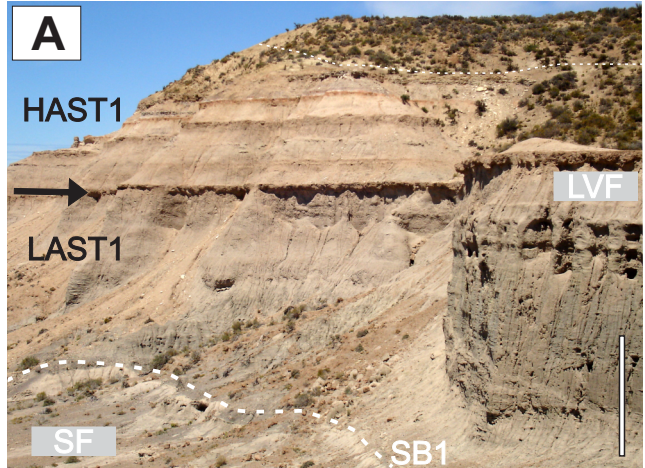
ESTANCIA LAS VIOLETAS



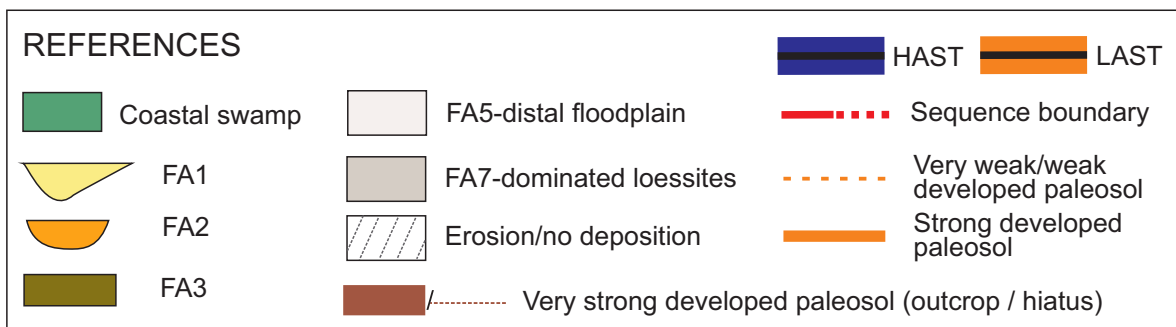
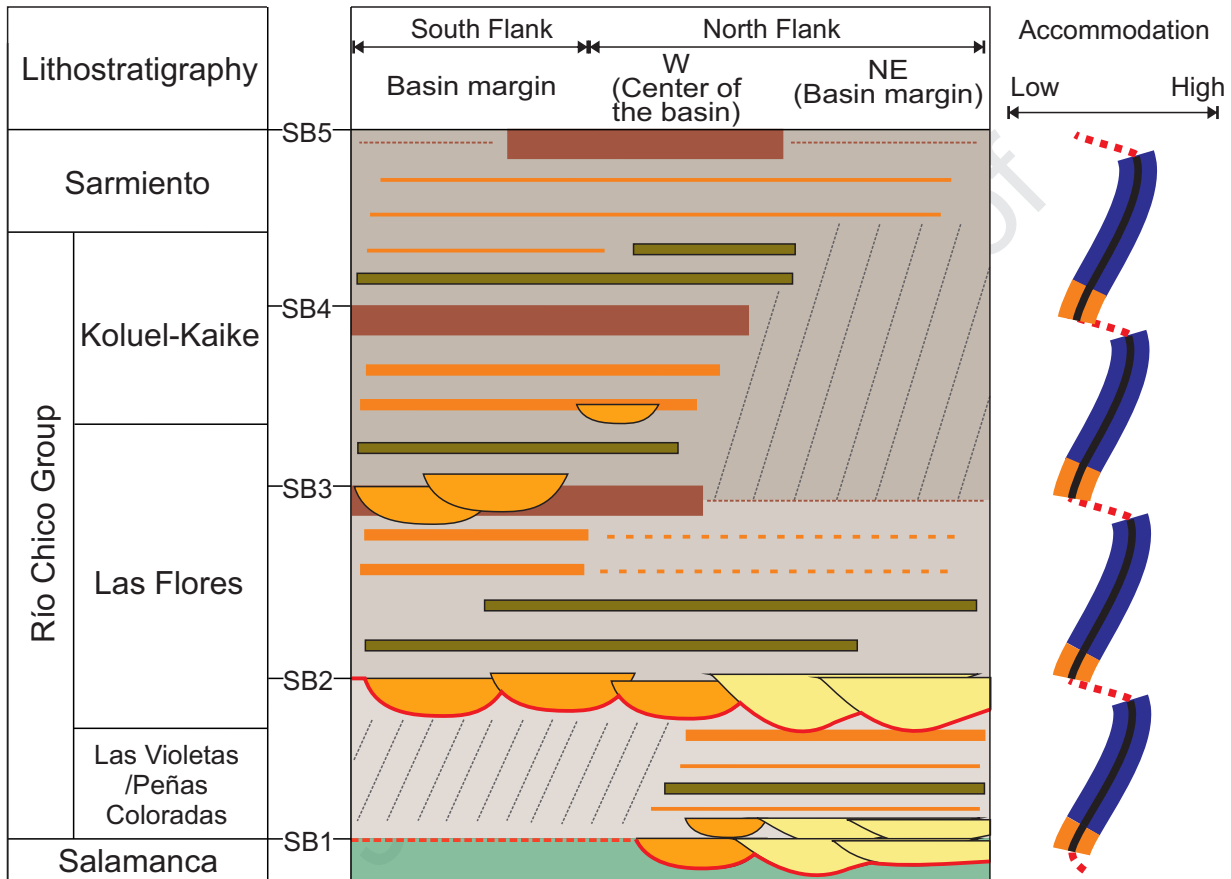
NE











Highlights

- Paleogene infill of the GSJB can be divided into 4 sequences.
- Sequence boundaries are related to fluvial incision or to mature paleosols.
- Mature paleosols reflect the transition from greenhouse to icehouse world.
- Accommodation space, base level and climate controlled system tracts evolution.
- Subsidence rates controlled fluvial architecture spatial variability.

Table 1: Summary chart of the facies associations identified in the Río Chico Group

Facies Association (FA)	Facies	Lithology	Color	Sedimentary features and paleosol type
Low-sinuosity fluvial channels (FA1)	Gm, Gt, Gp, Sm, St, Sp	Massive (Gm), trough cross-stratified (Gt) and planar cross stratified (Gp) tuffaceous conglomerates; and massive (Sm), trough cross-stratified (St) and planar cross stratified (Sp) coarse-grained to medium-grained sandstones with pumiceous clasts or intraclast	Greenish to grayish	Multiple and mobile channels
Moderate- to high-sinuosity fluvial channels (FA2)	Gm, Gt, St, Sp, Se, Sl	Massive (Gm) and trough cross-stratified (Gt) conglomerates; and trough cross-stratified (St), planar cross-stratified (Sp), epsilon cross-bedding (Se) and low-angle cross-stratified (Sl) coarse to medium-grained sandstones	Whitish or grayish to yellowish and pinky	Lateral and vertical amalgamation, large-scale inclined surfaces
Sheet-flood deposits (FA3)	Sm, Fm, TSm, TMb, TMm	Massive fine-grained sandstones (Sm), massive mudstones (Fm), massive tuffaceous sandstones (TSm), massive tuffaceous mudstones with intraclast at the base (TMb) and massive tuffaceous mudstones (TMm)	Gray to yellowish-orange	Tabular bodies, internally ungraded, erosive bases. Entisol-, Andisol-, Inceptisol-, Alfisol-, Ultisol, Ultisol-like paleosols with plinthitic horizon
Proximal floodplain deposits (FA4)	St, Sm, Sr, Sl	Trough cross-stratified (St), massive (Sm), ripple cross stratification (Sr) and laminated (Sl) medium- to fine-grained sandstones	Pinky to reddish	Crevasse splays and channel deposits. Entisol-like paleosols
Distal floodplain deposits (FA5)	Fm, Fl, TMm, Tm	Massive (Fm) and laminated (Fl) very fine-grained sandstones to mudstones, and massive to laminated very fine-grained tuffaceous sandstones to mudstones (TMm), massive very fine-grained tuffs (Tm)	Gray and white to pinky	Tabular bodies, great lateral extension. Entisol-, Andisol-, Inceptisol-, Ultisol-like paleosols
Low-hierarchy fluvial channels (FA-6)	TSt	Very poorly-preserved trough cross-bedding very fine-to fine-grained tuffaceous sandstones with intraclasts at the base (TSt)	White and light brown	Ribbon shaped bodies, single and low-sinuosity channels, laterally stables. Ultisol-, Ultisol-like paleosols with plinthitic horizon
Loessites (FA7)	TMm	Massive tuffaceous siltstones (TMm)	White, light gray and pale brown	Massive, broad sheets. Entisol-, Andisol-, Ultisol-, Ultisol-like paleosols with plinthitic horizon
Shallow ponded areas (FA8)	TMI	Poorly-preserved plane-parallel lamination to laminated tuffaceous siltstones-mudstones (TMI)	White to very pale brown	Narrow lenticular bodies. Andisol-, Inceptisol-like paleosols

Table 2: Summary of the most distinctive pedogenic features within the paleosol in the study area

Degree of development	Paleosol type	Main pedofeatures	Lithostratigraphic unit and Locality of occurrence	Author
Very weak and weak	Entisol-like	^{1,2} Rhizoliths, burrows, Fe-nodules, mottles, slickensides; ³ Burrows, relict primary stratification	LFF (Rocas Coloradas area) ^{1,2} ; KKF (Río Deseado area) ³	^{1,2} Raigemborn et al. (2009b) and Krause and Piña (2012); ³ Raigemborn et al. (2018a)
	Andisol-like	¹ Rhizoliths, burrows, granular structure, Mn-nodules	KKF (Las Flores area) ¹	¹ Krause et al. (2010a)
	Inceptisol-like	¹ Rhizoliths, Fe-nodules, mottles; ^{2,3} Rhizoliths, Fe-nodules, mottles, slickensides; ⁴ Blocky structure, rhizoliths, slickensides; ⁵ Rhizoliths, slickensides, Fe-nodules, Mn-nodules, platy structure	LVF (Estancia Las Violetas) ¹ ; PCF and LFF (Cerro Abigarrado and Las Flores area) ^{2,3} ; LFF (Cerro Blanco) ⁴ ; KKF (Río Deseado area) ⁵	¹ Krause et al. (2010b); ^{2,3} Raigemborn et al. (2009a and b); ⁴ Krause et al. (2017); ⁵ Raigemborn et al. (2018a)
Strong and very strong	Alfisol-like	¹ Rhizoliths, blocky and granular structures	LVF (Estancia Las Violetas) ¹	¹ Krause et al. (2010b)
	Ultisol-like	¹ Blocky structure, slickensides, Fe-nodules; ² Rhizoliths, Fe-nodules, irregular mottles, Fe-cutans, slickensides, blocky structure; ^{3,4} Rhizoliths, slickensides, Fe-nodules, irregular mottles, Fe-cutans, blocky structure	KKF (Las Flores area) ¹ ; KKF (Río Deseado area) ² ; LFF and KKF (Laguna Manantiales) ^{3,4}	¹ Krause et al. (2010); ² Raigemborn et al. (2018a); ^{3,4} Lizzoli et al. (2018) and Raigemborn et al. (2018b)
	^{1,2} Oxisol-like?			
	³ Laterite-like or ⁴ Plinthite-like or Ultisols with plinthitic horizon	^{1,2} Rhizoliths, Fe-reticulated mottles, blocky structure; ³ Fe-nodules, Fe-mottles, slickensides; ⁴ Rhizoliths, blocky and prismatic structures, Fe/Mn-nodules, slickensides, Fe-irregular and reticulated mottles	LFF (Laguna Manantiales) ^{1,2} ; KKF (Las Flores area) ³ ; KKF (Río Deseado area) ⁴	^{1,2} Lizzoli et al. (2018) and Raigemborn et al. (2018b); ³ Krause et al. (2010); ⁴ Raigemborn et al. (2018a)
	¹ Calcrete or Aridisol-like with calcrete horizon	¹ Petrocalcic horizons, rhizoliths, burrows	RM (Las Flores area) ¹	¹ Bellosi and González (2010)